# The influence of urban visuospatial configuration on older adults' stress: A wearable physiological-perceived stress sensing and data mining based-approach

Alex TORKU[1], Albert P. C. CHAN[2], Esther H. K. YUNG[3], JoonOh SEO[4]

[1]Department of Building and Real Estate, The Hong Kong Polytechnic University, 11 Yuk Choi Rd, Hung Hom, Kowloon, Hong Kong (corresponding author). Email: alex.torku@connect.polyu.hk Phone number: +852 5113 5350

[2]Department of Building and Real Estate, The Hong Kong Polytechnic University, 11 Yuk Choi Rd, Hung Hom, Kowloon, Hong Kong. Email: albert.chan@polyu.edu.hk

[3]Department of Building and Real Estate, The Hong Kong Polytechnic University, 11 Yuk Choi Rd, Hung Hom, Kowloon, Hong Kong. Email: esther.yung@polyu.edu.hk

[4]Department of Building and Real Estate, The Hong Kong Polytechnic University, 11 Yuk Choi Rd, Hung Hom, Kowloon, Hong Kong. Email: joonoh.seo@polyu.edu.hk

**Abstract**

Population ageing raises many fundamental questions, including how the urban environment can be configured to promote active ageing. The perceived element for older adults' involvement in the environment differs from the average person. Despite this difference, there is little to no research into understanding how the perceived elements (specifically, the visuospatial configuration) of the environment influence older adults' involvement—most studies focused on younger adults. The focus here is stress, which occurs when environmental demand exceeds a person's capability. As stress impacts a person's involvement in the environment and older adults are more likely to feel stress due to their decline in functional capability, it is important to understand how the visuospatial configuration of urban environment influence stress. Older adults were recruited to participate in an urban environment walk while their physiological responses (Photoplethysmogram) were monitored using wearable sensors. Their perceived stress responses were also collected. Spatial clustering and hot spot analysis were conducted to detect locations with clusters of physiological responses caused by spatial factors. These locations were subsequently labelled as stress or non-stress based on participants' perceived stress. The perceived visual elements of the urban environment were extracted using isovist analysis. Principal component analysis, self-organising map and machine learning algorithms were used to understand the relationship. The results demonstrate that isovist minimum visibility, occlusivity, and isovist area are the most influential determinants of older adults' physiological stress. Older adults prefer urban configurations where they can be seen. This study can be used to inform urban design and planning.

## 1. Introduction

The age structure of today's population shows that the world is experiencing an unparalleled phenomenon in terms of ageing. The share of the people in the global population aged 65 and over is projected to increase from 9.3% in 2020 to 16.0% in 2050. Globally, one in six people is expected to age 65 years by 2050 (United Nations, 2020). In view of an ageing population, governments worldwide have been stepping up efforts to promote active ageing. Active ageing is a concept developed by the World Health Organisation (WHO), which emphasises creating an enabling environment for older adults to continue participating in social, economic, civic engagement and physical activity in order to enhance their quality of life as they age (WHO, 2018; Torku et al., 2020). The older adult's mobility—their ability to achieve access to their desired places (physical environment) and people (social environment)—is critical for such an enabling environment (referred to as age-friendly cities and communities) to adequately function. Mobility is essential to accessing commodities, using neighbourhood facilities, engaging in social, cultural, and physical activity; thus, fundamental to active ageing (Rantanen, 2013).

Mobility limitation is not entirely due to ageing but the interaction between an individual and his or her environment (Webber et al., 2010; Verbrugge, 2020; WHO, 2001). Mobility limitation arises for an activity when there is a gap between personal capability and the activity's demand (Verbrugge and Jette, 1994). The two main interventions to promote mobility is either by

3

increasing capability or reducing demand. Interventions to increase or maintain an individual's capacity are made by the individual or medical professionals. Recommended options to reduce demand are activity accommodation, environmental modifications, psychosocial coping, and external support (Verbrugge and Jette, 1994; Verbrugge, 2020). This study focuses on the modification of the built environment to reduce environmental demand. Environmental demand is the collective influence of elements constituting the environment to produce expectations for certain human actions and reactions (Hagedorn, 2001; Lee et al., 2020). When environmental demand meets a person's capability, the person can achieve successful mobility. On the other hand, the person experience stress and/or their mobility is limited when the environmental demand exceeds their capability (Mair et al., 2011; Yang and Matthews, 2010; Lawton, 1982; Webber et al., 2010).

Stress is a type of relationship between person and environment which occurs when demands tax or exceed the person capability (Lazarus, 1990). When a person appraises an encounter as stressful, the coping process is initiated to manage the troubled person-environment relationship; these processes influence the person's subsequent appraisal and reaction to such stressful encounters (Lazarus, 1990). Given that an individual's functional capability increases in childhood, peaks in early adulthood, and eventually decline (WHO, 2007; Kalache and Kickbusch, 1997), it is more likely for older adults to experience stress in the urban environment than other age groups. In fact, recent studies have reported that the desire to reduce encounters with stressful environmental conditions has led to a significant reduction in mobility of older adults in the built environment (van Heezik et al., 2020; Portegijs et al., 2017). As a result, there has been a rapid decline in mobility indices, including trip frequency, trip distance, and unmet travel demands among older

adults (Shumway-Cook et al., 2003; Portegijs et al., 2017). In a sense, this may indicate that the perceived element for older adults' involvement in the environment might differ from that of the average person (Gibson, 1977; Chemero, 2003). Therefore, there is an urgent need to understand the influence of perceived elements of the urban environment on older adults.

## 1.1. Visuospatial perception

For sighted individuals, spatial information acquisition occurs largely through their sense of vision (Kiefer et al., 2017). The spatial properties of the environment as perceived through the eyes are referred to as the visuospatial properties of the environment. The visuospatial properties of the environment are influenced by two main elements: the surface characteristic and appearance (e.g., material, texture, and colour) and the configuration (e.g., arrangement and size) of the spatial forms (Schneider and Koenig, 2012). This study considers only the visuospatial configurations of the environment.

In the broader environmental psychology literature, several theories have emphasised that human behaviour and experience are determined by the properties of the spatial form of the environment. For example, the prospect-refuge theory discovered by Appleton (1975) postulates that humans prefer a spatial configuration that affords both the ability to see (prospect) without being seen (refuge). "Where these conditions are present their perception is attended with pleasure; anxiety is set aside and relaxation is possible. Where they are absent anxiety continues and there is no relaxation" (Appleton, 1975, p. 71). Akin to the prospect-refuge theory is the defensible space theory that suggests that the environment can be configured to influence its residents' territoriality, image, milieu, and surveillance behaviours (Reynald and Elffers, 2009). The mystery

theory propounded that humans behavioural and emotional responses are influenced by spatial configurations promising new information when proceeding further into the environment (Kaplan, 1988). The complexity concept suggests that human involvement (the concern to figure out, to learn, to be stimulated) in an environment is affected by the diversity or richness (how much there is to look at) in the environment (Kaplan, 1988; Scott, 1993). These theories have been evaluated on several architecture spaces (including Frank Lloyd Wright's architecture) and urban space (Dawes and Ostwald, 2014; Wu et al., 2020; Franz and Wiener, 2005; Xiang et al., 2020). The theories collectively suggest that the human visuospatial perception of a space generated by or associated with a spatial configuration affects human behaviour and experience; this effect on humans is an important factor for creating and maintaining a liveable environment (Gehl, 2011).

The human visuospatial perception of a horizontal slice through space can be measured using isovist analysis. It is important to mention that other methods, including the traditional self-report assessment, spatial cognition analysis and tests in immersive virtual and augmented reality environments, have been used to assess human interaction with the spatial environment (Ergan et al., 2019; Kiefer et al., 2017; Banaei et al., 2017; Shemesh et al., 2017). In this study, visuospatial perception is quantified using isovist. An isovist is a space in an environment visible to a person from an observation point from which various geometrical and mathematical measures are computed to define the person's visuospatial perception (Benedikt, 1979; Batty, 2001). Isovist can be studied in both two and three dimensions (Giseop et al., 2019). This study is limited to the two-dimensional isovist analysis. Isovist analysis is capable of describing a space "'from inside', from the point of view of individuals, as they perceive it, interact with it, and move through it" (Turner et al., 2001, p.103). Isovist analysis has been widely used in the fields of architecture and urban

planning in the study of wayfinding (Meilinger et al., 2012), visibility (Wu et al., 2020), Prospect-Refuge Theory (Dawes and Ostwald, 2014; Ostwald and Dawes, 2013) and urban emotion (Li et al., 2016; Knöll et al., 2018; Xiang et al., 2020). Pertinent isovist research has shown that several geometrical and mathematical measures (referred to as isovist indicators): area, perimeter, compactness, occlusivity, jaggedness, maximum visibility, and minimum visibility (Benedikt, 1979; Batty, 2001; Schneider and Koenig, 2012) are to some extent associated with spatial perceptions including those relating to elements of prospect, refuge (in the prospect-refuge theory), mystery (in the mystery theory), and complexity (in the complexity theory). These isovist indicators and the experiential properties associated with them are presented in Table 1.

Isovist area represents the area of all spaces visible from a person's observation point. Isovist perimeter measures the length of the edge of all space visible from an observation point. Compactness expresses the relationship between area and perimeter relative to a circle; it indicates the complexity or compactness of the field of view (Schneider and Koenig, 2012). Occlusivity describes the length of open edges (i.e., edges without physical boundaries such as a wall) of the field of view (Dawes and Ostwald, 2014). Occlusivity is small in locations with few or no views into other parts of the spatial configuration of the environment. For instance, an observation point within a completely closed, convex space has an occlusivity of 0. Jaggedness describes the convexity (i.e., the number of vertices and vertex density) of the field of view (Wiener and Franz, 2004). The maximum visibility and minimum visibility refer to the length of the longest and shortest single view, respectfully, available at an observation point.

Table 1. Isovist indicators with corresponding experiential properties.

| Isovist indicator | Spatial experience | Spatial property | References |
|---|---|---|---|
| Isovist area | Prospect | Spaciousness | Chun et al. (2019), Ostwald and Dawes (2013), Dawes and Ostwald (2013), Franz and Wiener (2005), Xiang et al. (2020), Reynald and Elffers (2009), Dawes and Ostwald (2014), Wu et al. (2020) |
| Isovist perimeter | Prospect | Spaciousness | |
| Maximum visibility length | Prospect | Spaciousness | |
| Minimum visibility length | Refuge | Spaciousness | |
| Occlusivity | Refuge | Openness | |
| Occlusivity | Mystery | The promise of more information | Dawes and Ostwald (2013), Benedikt (1979), Kaplan (1988), Xiang et al. (2020), Dawes and Ostwald (2014) |
| Jaggedness | Complexity | Diversity or richness | Dawes and Ostwald (2013), Kaplan (1988), Scott (1993), Franz and Wiener (2005), Wiener and Franz (2004), Xiang et al. (2020), Ma et al., (2020) |
| Compactness | Complexity | Diversity or richness | |

## 1.2. Research aim and significance

A few studies have been conducted to understand the relationship between the visuospatial configuration of urban space and human physiological response (Li et al., 2016; Hijazi et al., 2016; Knöll et al., 2018; Ojha et al., 2019; Xiang et al., 2020). All of these studies focused on younger adults with an average age of about 25 years. Drawing on these findings to guide urban planning and design may discriminate against older adults even though they are more susceptible to stressful urban environment encounters. This could further hinder current efforts in creating universal designs and age-friendly cities and communities.

In the previous studies, human physiological responses were generally categorised into positive and negative emotions (Li et al., 2016; Hijazi et al., 2016; Xiang et al., 2020); normal and aroused physiological response (Ojha et al., 2019); and not stressful and maximum stressful (Knöll et al.,

2018). Categorising physiological responses into positive and negative emotions or normal and aroused physiological responses is too broad and may not provide an adequate understanding of the person-environment relationship. For instance, feeling excited and calm are different types of positive emotions, and feeling stressed and bored are different types of negative emotions (Barrett and Russell, 1998; Scherer, 2005); therefore, it will be difficult to understand which spatial configuration is eliciting a specific emotion. Knöll et al.'s (2018) study indicates that a specific emotion (i.e., stress) can be detected to understand the person-environment relationship. Knöll et al.'s (2018) approach is based on perceived stress rating (i.e., user's rating of an urban environment as stressful or not). However, the perceived stress rating may not be entirely accurate in detecting actual environmental stress spots because of the subjectivity of individual reported perception (Aghaabbasi et al., 2018). As a result, perceived stress reports can be mixed up with several stress stimuli encountered in people's daily trips. The main advantage of this approach is that it can be easily used to estimate urban stress and non-stress person-environment relationship (Rishi and Khuntia, 2012; Knöll et al., 2018).

Physiological responses have been used to detect stress during real-world settings. For example, Healey and Picard (2005) detected stress during real-world driving tasks using physiological responses. Physiological responses combined with spatial analysis have been used to detect stress in ambulatory, outdoor or built environment settings (Li et al., 2016; Chrisinger and King, 2018; Birenboim et al., 2019; Kim et al., 2019; Lee et al., 2020; Saitis and Kalimeri, 2021). However, results from the physiological responses sensed in an ambulatory, outdoor or built environment are inconsistent. For instance, Chrisinger and King (2018) reported that physiological response was higher in favourable (non-stressful) environmental conditions and lower in less favourable

(stressful) environmental conditions. Whereas Lee et al. (2020) reported high intense physiological responses at built environmental conditions with barriers (stressful conditions) and low intense physiological responses at built environmental conditions without barriers (non-stressful conditions). This means that either high or low physiological responses can indicate environmental stress and non-stress spot. The main advantage of this approach is that the data is user-centred, objective and can be combined with spatial analysis to minimise the impact of random environmental factors on stress (Li et al., 2016; Kim et al., 2019).

To understand the influence of spatial factors on stress, it is important to distinguish stressful person-environment interactions due to spatial factors from stressful person-environment interactions due to other environmental or personal factors. In this study, the authors harness the advantages of the perceived stress rating and the physiological responses stress detection (physiological-perceived stress). The aim is to (1) estimate stress and non-stress environmental conditions using perceived response (2) integrate physiological response with GPS data, conduct hot spot analysis to identify hot spots and cold spots (3) spatially match hot spots and cold spots to perceived response to detect stressful person-environment interactions due to spatial factors in order to enhance our understanding of the relationship between the visuospatial configuration of urban space and older adults stress response. Given the rate of population ageing and the likelihood of older adults encountering excessive environmental demands during their daily trips, this research is important to efficiently understand their relationship with the environment to inform urban planning and design. The research overview is presented in Fig. 1.
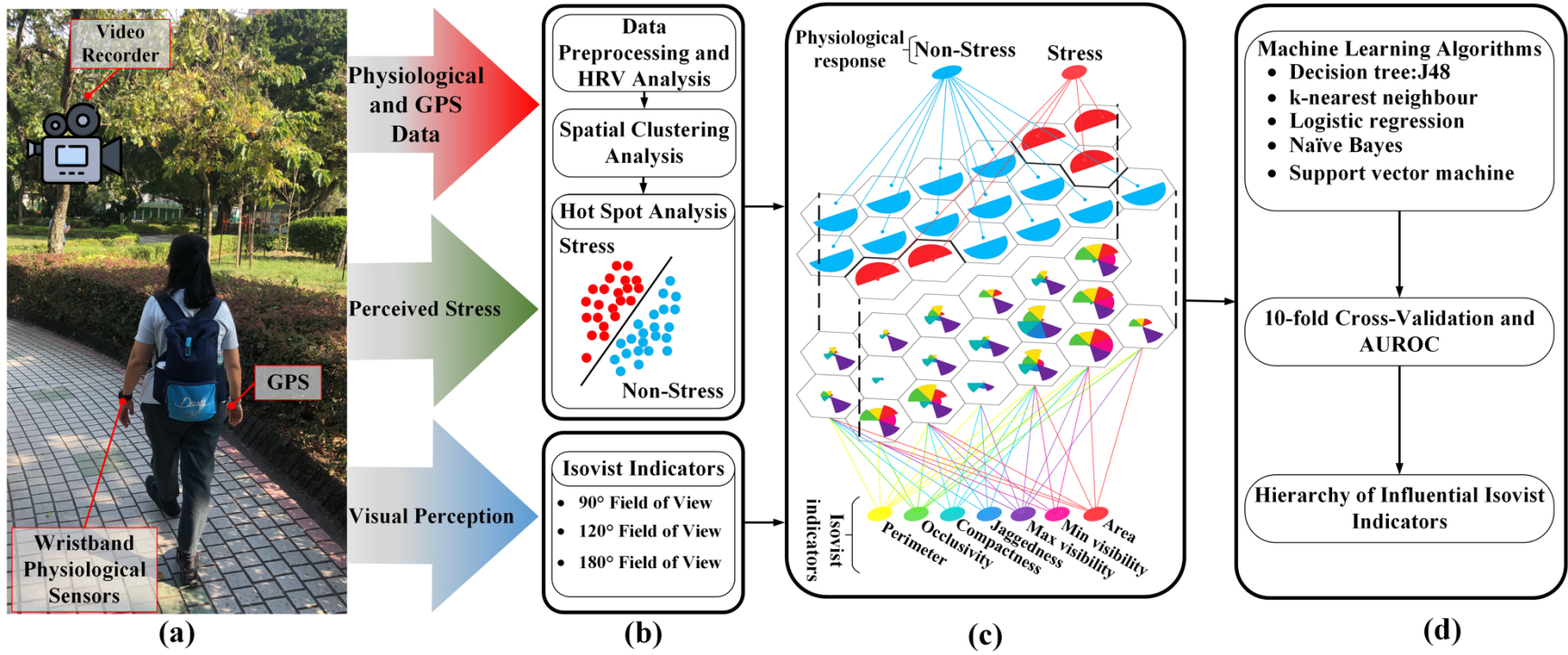
Fig. 1. Overview of research. (a) Data collection during an environmental walk. (b) Data processing, heart rate variability (HRV) analysis, hot spot analysis, and computing isovist indicators from different fields of view. (c) Self-organising Maps depicting the influence of visual perception on physiological response. (d) Adopting machine learning algorithms to identify the most influential isovist indicators of physiological response. The performance of the algorithms was examined using the Area under the Receiver Operating Characteristic (AUROC) based on 10-fold cross-validation.

## 2. Method

### 2.1. Experiment design and data collection

The field data collection was conducted in the neighbourhood of Hung Hom, Kowloon, Hong Kong. A total of ten older adults (Table 2) were recruited to participate in an environmental walk on a 570 m predefined path. The path was chosen because it captures a range of spatial configurations, including spacious and narrow streets, high and low-density building areas, as shown in Fig. 2. The path is located in an old district currently undergoing urban renewal. All participants achieved a score of ≥ 22 points on the Cantonese version of the Mini-Mental State Examination. A cut-off score of 19/20 is recommended to indicate cognitive impairment among Hong Kong older adults (Chiu et al., 1998; Lao et al., 2019). Only one participant (participant 7) used a walking stick for mobility. None of the participants has previously experienced or is familiarised with the path. This study should be interpreted bearing in mind that the survey is female-dominated, and there were no people over 76 years of age. The median age of the participants is 66, which is just the retirement age in many countries. The environmental walk was conducted in November 2019 between 10 a.m. and 4 p.m. The environment temperature ranges from 24°C-29°C, and the humidity ranges from 41%-55%. The participants completed and signed an informed consent form after obtaining written and spoken information about the experimental procedure. A shopping voucher of HK$100 was offered as compensation for participation. The predefined path and the experimental procedures were reviewed and approved by the Human Subjects Ethics Sub-committee of The Hong Kong Polytechnic University (Reference Number: HSEARS20190826002).

Table 2. Demographic information of participants.

| Participant | Gender | Age (years) | Height (cm) | Weight (kg) | Body mass index (kg/m$^2$) | Time to walk the path (MM: SS) |
|---|---|---|---|---|---|---|
| 1 | Female | 65 | 162.0 | 57.0 | 21.7 | 11: 31 |
| 2 | Female | 65 | 158.0 | 62.0 | 24.8 | 8: 47 |
| 3 | Male | 66 | 160.0 | 71.0 | 27.7 | 9: 59 |
| 4 | Female | 75 | 161.1 | 67.5 | 26.0 | 8: 55 |
| 5 | Male | 68 | 173.0 | 83.0 | 27.7 | 13: 47 |
| 6 | Female | 72 | 157.5 | 54.4 | 21.9 | 9: 56 |
| 7 | Female | 71 | 152.4 | 60.5 | 26.0 | 15: 01 |
| 8 | Female | 66 | 157.5 | 59.0 | 23.8 | 10: 57 |
| 9 | Female | 66 | 154.9 | 60.0 | 25.0 | 8: 57 |
| 10 | Male | 66 | 175.0 | 77.7 | 25.4 | 9: 00 |

The environmental walk was completed in two phases. During the first phase, the participants walk the path in one direction (i.e., from start to finish, as shown in Fig. 2) at a self-directed pace to optimise their experience and enable ecological validity. While walking along the path and experiencing the environment, the participants' physiological response—Photoplethysmogram (PPG) signal at 64 Hz—were collected using a wristband-band type sensor (Empatica E4). The participants also wore a belt-clip-type Global Positioning System (GPS) sensor (Qstarz BT-Q1000XT) for geographical referencing (at 1 Hz). The participants' environmental walk was video recorded. Two researchers accompanied the participants. One of the researchers was present for safety and health purposes. The other researcher recorded a video of the environmental walk. The accompanied researchers remained half a stride behind the participants to allow the participants to determine the pace. Upon completing the first phase of the environmental walk, the participants walked the same path without wearing the sensors. Instead, a survey was conducted while the participants were walking. Each participant was asked to identify the locations on the path where they experienced stressful interactions with the environment. The participants also stated the intensity of their perceived stress (low or high intensity). A researcher accompanied and assisted

the participants in documenting their responses. This approach was adopted to ensure that older

adults accurately recall their experiences.



Fig. 2. Path with perceiver's view in the forward direction, starting from A to L. Basemap data copyrighted Esri, DigitalGlobe, GeoEye, Earthstar Geographics, CNES/Air bus DS, USDA, USGS, AeroGRID, IGN, and the GIS User Community. Photographs by authors.

**2.2. Detecting stress and non-stress responses to the urban environment: Perceived and Physiological**

The commonality in the participants perceived responses are analysed. The path is categorised into (1) stress (high or low) and (2) non-stress based on the commonly perceived responses. In this study, the commonly perceived response is considered an estimation of urban stress and non-stress spots. The perceived response is complemented with physiological response to minimise the impact of stress due to random or personal factors and maximise the impact of stress due to spatial factors. The following outlines the pre-processing and spatial analysis of the physiological response.

Stress—either environmental or psychological—triggers several stress hormones that result in human physiological changes (Kogler et al., 2015). The general response to stress activates the autonomic nervous system (ANS) (Acharya et al., 2006). PPG signal contains valuable physiological information; it reflects a changing arterial wave during each cardiac cycle which is influenced by the ANS (Heo et al., 2021; Charlton et al., 2018). Aside from the informativeness of the PPG signal, it is collected by attaching sensors to the wrist; therefore, it is a non-invasive and less obstructive means of monitoring older adults' physiological responses during a real-world ambulatory setting. Heart rate variability (HRV) is a reliable signal for understanding the status of the ANS (Acharya et al., 2006). Previous studies have used HRV metrics to distinguish between normal and stressed states (Kabisch et al., 2021; Birenboim et al., 2019; Healey and Picard, 2005; Saitis and Kalimeri, 2021).

Before extracting the HRV metric, the recorded video of each participant's environmental walk was inspected by the authors and unintended person-environment interaction (e.g., older adults interaction with vehicles, people, and losing stability due to encounters with path obstructions such as potholes, stairs, or curbs) that could affect stress were excluded to ensure that the physiological response was mainly influenced by spatial factors. To extract the HRV metric, the authors computed the inter-beat interval (IBI) from the PPG signal. The IBI is the time interval between individual beats of the heart. IBI was used to estimate the instantaneous heart rate at 1 Hz using a proprietary algorithm (Empatica, 2020). Artefacts including missing, extra, or misaligned beats and ectopic beats such as premature ventricular contractions or other arrhythmias were corrected, and HRV analysis was conducted, respectively, from the instantaneous heart rate using a proprietary algorithm (Tarvainen et al., 2014). All participants physiological responses were baseline normalised using 10 min baseline measurements to reduce inter-individual variability.

The balancing act of the sympathetic and parasympathetic components of the ANS controls the heart rate. The sympathetic component modulates heart rate at low frequencies ranging from 0.04 to 0.15 Hz, and the parasympathetic component modulates heart rate at high frequencies ranging from 0.15 to 0.4 Hz (Acharya et al., 2006). By computing the ratio of the low-frequency heart rate absolute spectral power to high-frequency heart rate absolute spectral power, the authors derived a HRV feature representing the ratio of the sympathetic to parasympathetic (sympathovagal balance) influence on the heart. The absolute spectral power of the low frequency (LF) band (0.04-0.15) and high frequency (HF) band (0.15-0.4) were calculated, and the ratio $LF/HF$ was derived. This $LF/HF$ ratio was used to model older adults' physiological stress responses to urban environmental conditions.

It is known that the expected physiological effect of a stressor occurs slightly after the stimulus (Healey and Picard, 2005). Therefore, the authors expect that the physiological effect of a stressful environmental condition would occur slightly after older adults interact with the environmental condition. The $LF/HF$ metric was extracted from a 60 sec response window in order to model the physiological effect of the environmental conditions accurately. Previous studies have reported that a 60 sec window produces informative HRV metrics (Shaffer and Ginsberg, 2017). To create a continuous $LF/HF$ metric that is proportional to the participant's physiological state throughout the environmental walk, the authors used the 60 sec response window, advanced by 1 sec for each second of the walk (to correspond to the 1 Hz GPS data) for the total duration of the environmental walk.

A participant experiencing a high or low physiological response at a location could result from spatial factors (e.g., spatial configuration), temporal factors (e.g., noise level and weather) or individual factors (e.g., health condition and previous experience). Because the participants' responses to the environment were collected on different days and different time-of-day, there was no direct mutual interference between them; therefore, it is assumed that their responses were comparatively independent. As a result, the authors employed spatial clustering analysis, specifically hot spot, to amplify the physiological responses induced by spatial factors while reducing the impact of temporal and random factors. Hot spot analysis was performed using Getis-Ord Gi* statistics to detect locations in the study area that elicited a common physiological response among multiple participants. Getis-Ord Gi* statistics is a useful GIS-based tool for detecting statistically significant spatial clusters of high values (hot spots) and low values (cold spots) (Ord and Getis, 1995). Previous studies have successfully used Getis-Ord Gi* statistics to

conduct spatial clustering on physiological data (Li et al., 2016; Chrisinger and King, 2018). The Getis-Ord Gi* statistics returns a z-score and a p-value for each physiological response experienced on the path by each participant. The resultant z-scores and p-values show the statistically significant spatial clusters of all participants' high or low physiological responses. A location is determined as a hot spot if the physiological response at that location is high and the physiological responses at the neighbouring locations are also high, and *vice versa* for a cold spot. The Getis-Ord Gi* statistics (Ord and Getis, 1995) is given as

$$G_i^* = \frac{\sum_{j=1}^{n} w_{i,j} x_j - \bar{X} \sum_{j=i}^{n} w_{i,j}}{S \sqrt{\frac{\left[ n \sum_{j=1}^{n} w_{i,j}^2 - \left( \sum_{j=1}^{n} w_{i,j} \right)^2 \right]}{n-1}}}, \tag{1}$$

where $x_j$ is the attribute value for physiological response $j$, $w_{i,j}$ is the spatial weight between physiological response $i$ and $j$, $n$ is equal to the total number of physiological responses, and

$$\bar{X} = \frac{\sum_{j=1}^{n} x_j}{n}, \tag{2}$$

$$S = \sqrt{\frac{\sum_{j=1}^{n} x_j^2}{n} - (\bar{X})^2}. \tag{3}$$

The detected hot spots and cold spots are spatially matched with the commonly perceived stress and non-stress path segments. The hot spots and cold spots within perceived stress path segments were detected as spatial significant stress locations, and hot spots and cold spots within the perceived non-stress path segments were detected as spatial significant non-stress locations.

**2.3. Measuring visuospatial perception: Isovist analysis**

The spatial layout of the experiment neighbourhood (Hung Hom, Kowloon, Hong Kong) was generated using OpenStreetMap (OpenStreetMap and Contributors, 2019), as shown in Fig. 3(a). The isovist was generated using DepthmapX (SpaceGroupUCL, 2019). DepthmapX has the following field of view options: 90°, 120°, 180°, and 360°. The combined visual field for both human eyes is 130-135° vertically and 200-220° horizontally (Szinte and Cavanagh, 2012; Dagnelie, 2011). During the environmental walk, the participants walked the path in one direction (i.e., from start to finish, as shown in Fig. 2); therefore, the maximum horizontal visible urban space to the participants is about 220°. Due to the limited field of view options available in DepthmapX, only the 90°, 120°, and 180° fields of view were used for the isovist analysis. Hence, the far peripheral vision of the human eye beyond 180° was ignored in this study. An example of the generated 90°, 120°, and 180° fields of view from an observation point on the path is presented in Fig. 3(b), Fig. 3(c), and Fig. 3(d), respectively. In order to capture a more realistic isovist, a view distance of 200 m was set, considering the visual acuity for an average 65-year-old. For instance, it would be unrealistic to assume that people have near-infinite isovists in an open space. Fig. 3(b) depicts a more realistic isovist with a visibility boundary from an observation point. The isovist within the visibility boundary represents a closed polygon from which isovist indicators: area, perimeter, compactness, occlusivity, jaggedness, maximum visibility, and minimum visibility were calculated. The isovist was generated for the entire path using the fields of view, the view distance, and the GPS locations as observation points. Isovist area is calculated as the total space bounded by the edges of the polygon, isovist perimeter is calculated as the total length of the edges of the polygon, isovist maximum and minimum visibility are calculated as the length of the longest and shortest line to the solid edge of the polygon from an observation point. The formulas for compactness, occlusivity, and jaggedness are

$$Compactness = 1 - \frac{2\sqrt{\pi S}}{P},$$ (4)

$$Occlusivity = P - P_f,$$ (5)

$$Jaggedness = \frac{P^2}{S},$$ (6)

where $S$ is the isovist area, $P$ is the isovist perimeter, and, $P_f$ is the total length of the solid edges within the isovist area ($S$).
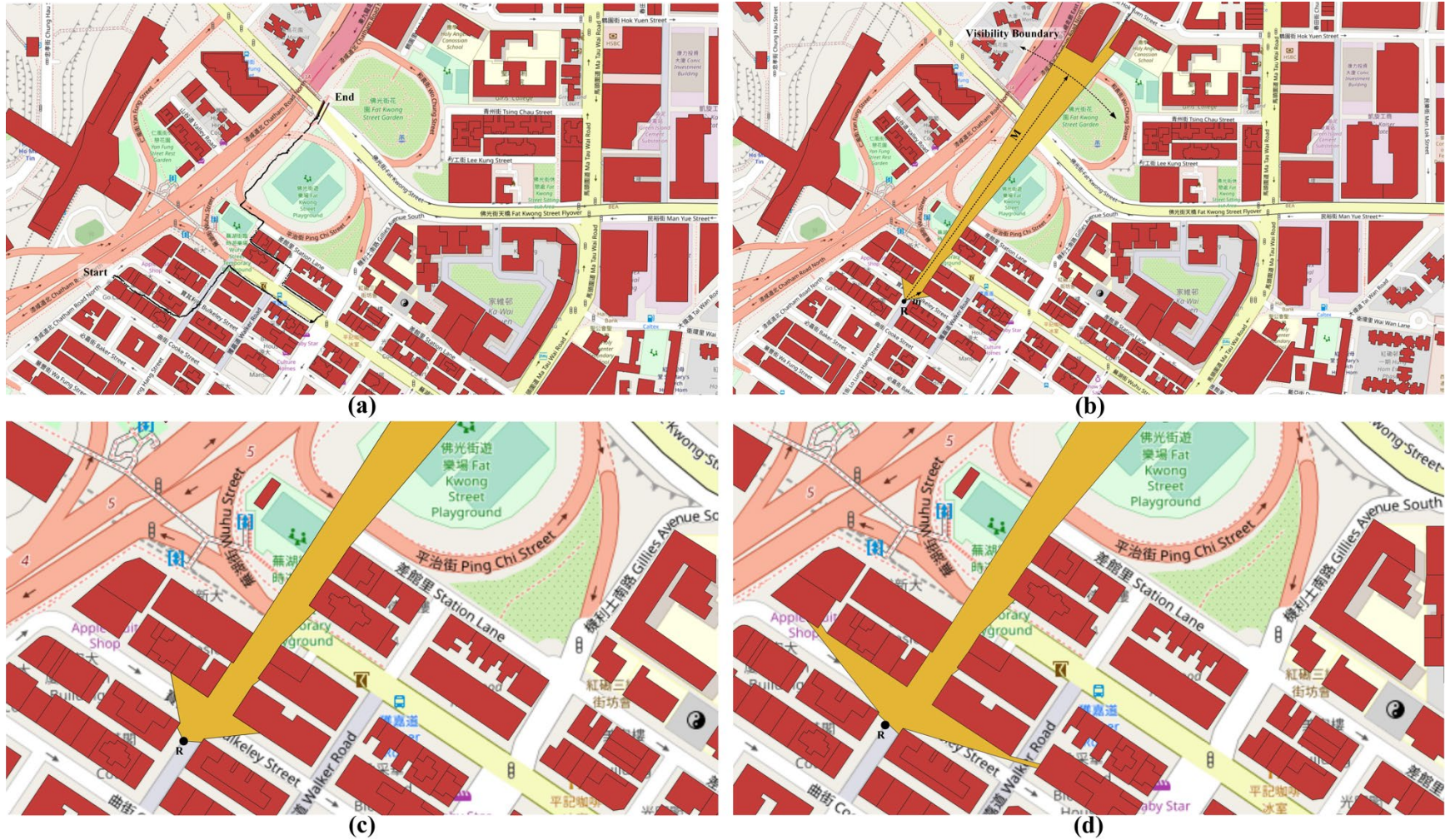
Fig. 3. Generated spatial layout with isovist from an observation point. (a) Spatial layout of the experiment neighbourhood with predefined path. (b) Isovist with 90° field of view from an observation point $R$ with a defined boundary, $M$ = visibility limit of 200 m (equivalent to the maximum visibility length), $m$ = minimum visibility length. (c) Isovist with 120° field of view from an observation point $R$. (d) Isovist with 180° field of view from an observation point $R$. Basemap data copyrighted OpenStreetMap (and) contributors.

**2.4. Influence of visuospatial perception on physiological response: Self-organising map**

A self-organising map (SOM) is a type of artificial neural network trained using unsupervised learning to visualise and explore different patterns and relationships in the data (Kohonen, 2013). SOM has a unique property of effectively projecting input space (high-dimensional space) into a low-dimensional (usually two-dimensional) regular grid such that the proximity relations are preserved (Vesanto and Alhoniemi, 2000). Maps that are generated using unsupervised SOM mainly capture the significant factors that influence the similarities in the data (e.g., clustering in the data). In this study, the authors are more interested in variations in factors resulting in a specific effect (i.e., the isovist indicators that influence physiological response). Supervised SOMs offer the opportunity to study the isovist indicators influencing physiological response by increasing their importance on the organisation of the maps (Platon et al., 2017; Wongravee et al., 2010; Kuzmanovski et al., 2007).

The SOM architecture is described in the following. Note that three different fields of view were considered in this study. Therefore, a SOM of two-dimensional grid size $M \times N = U$ nodes was generated for each field of view dataset. The input data $\mathbf{X}$, to be projected on the SOM of dimension $I \times J$ (which is $3283 \times 7$ for each field of view) and its label $\mathbf{Y}$ has dimensions $I \times K$ (where $K = 2$, representing the two classes of the physiological response [stress and non-stress]). The SOM learning process is as follows. Given a set of samples $(\mathbf{x}_i, \mathbf{y}_i)$ from the dataset $(\mathbf{X}, \mathbf{Y})$, $i = 1, \cdots, n$, where $\mathbf{x}_i$ is the input vector of the $i$th sample and $\mathbf{y}_i$ is a vector corresponding to its label (recall that the dimension of $\mathbf{y}_i$ is equal to the number of classes in the label, which is 2 in this study). If the class of $\mathbf{x}$ is $l$, the $l$th component of $\mathbf{y}_i$ is equal to 1 and the other component is equal to 0. The supervised SOM is able to learn a function $f : \mathbf{X} \rightarrow \mathbf{Y}$ by training on an augmented vector $\mathbf{x} =$

$[x_v, x_l]$, which is a combination of label vector $x_l$ with the input vectors $x_v$. Each node $r$, in the supervised SOM has a weight vector $w_r = [w_r^v, w_r^l]$. During the competitive learning process, the distance between $x_i$ and $w_r$ of each node is computed. The best matching unit (BMU) is determined by finding the node $r$, having the closest weight vector $w_r$, to the input vector $x_i$:

$$b = \arg\min_r d(x_i, w_r), \tag{7}$$

where $b$ denotes the index of the BMU and $d(x_i, w_r)$ is the Tanimoto distance between $x_i$ and $w_r$ (note that the **Y** is categorical, hence the reason for using Tanimoto distance measure). The BMU and its topological neighbours are updated as

$$w_r(t + 1) = w_r(t) + \alpha(t)h_{br}[x_i - w_r(t)], \tag{8}$$

where $\alpha(t)$ is the learning rate at time $t$—$\alpha(t)$ is a monotically decreasing function—and $h_{br}$ is the neighbourhood function between BMU and the $r$th node at time $t$. The two traditional neighbourhood functions are the bubble function and Gaussian function. Both neighbourhood functions were tested. The learning process adopted in this study is based on the classical sequential SOM algorithm (Kohonen, 2013). The learning process is repeated until there is convergence in **X** and **Y**. Several SOM were trained in parallel using different hyperparameters settings. The optimal SOM was selected using the Area under the Receiver Operating Characteristic (AUROC) based on 10-fold cross-validation. The AUROC and the validation of the SOM are explained in the validation section.

**2.5. Identifying the most influential isovist indicators of physiological response**

The SOM is able to provide the isovist indicator levels that are responsible for stress and non-stress physiological responses. However, it is also important to ascertain which of the isovist indicator (s) have the greatest influence on older adults' physiological responses. Hence, subsets of isovist indicator (s) based on their correlation and intercorrelation were generated. Subsets of isovist indicator (s) that are highly correlated with the physiological responses, while having low intercorrelation, have greater influence (Hall, 1999). A greedy forward search was performed through the space of the generated subsets to create a hierarchy of influential isovist indicator (s) subsets. A greedy forward search is an efficient method to select a choice from multiple choices that achieve the largest possible improvement or fitness in the value of some measure (Resende and Ribeiro, 2010).

The hierarchy of influential subsets of isovist indicator (s) was subsequently confirmed by considering its ability to discriminate between stress and non-stress physiological responses when used to train several machine learning algorithms. Decision tree (J48), k-nearest neighbour (kNN), logistic regression, Naïve Bayes, and support vector machine were used because they have been successful used in previous studies to detect stress (Panicker and Gayathri, 2019). The performance of the algorithms was examined using the Area under the Receiver Operating Characteristic (AUROC) based on 10-fold cross-validation.

**2.6. Validation**

k-fold cross-validation (k = 10) was used to evaluate the performance of the SOM and the machine learning algorithms. Cross-validation is a resampling procedure that has been widely used in

machine learning to estimate the skill of a model on unseen data (Bengio and Grandvalet, 2004). k-fold cross-validation involves randomly splitting the original sample data into k groups of approximately equal size. One group out of the k groups is held out to validate the model, and the remaining k-1 groups are used to train the model. The training and validation are repeated k times to calculate the performance of the model on the validation data set. The value of k = 10 was used for the cross-validation; this value has been proven to produce validation results that suffer neither from excessively high bias nor from very high variance (James et al., 2013).

The performance of the models was evaluated using the Area Under the Receiver Operating Characteristic (AUROC). The Receiver Operating Characteristic (ROC) curve is constructed by plotting the model's true positive rate (sensitivity) against the false positive rate (1-specificity) at various threshold settings. AUROC is a performance metric for discrimination; it indicates a model's ability to discriminate between positive and negative cases (Brown and Davis, 2006). An AUROC of 1.0 corresponds to a perfect performance; the lower the AUROC, the worse the performance. In general, AUROC above 0.5 indicates good performance, whereas AUROC below 0.5 indicates poor performance. The model with the highest AUROC value was selected as the optimal model.

## 3. Results

### 3.1. Detected stress and non-stress responses to urban environment: Perceived and Physiological

All participants reported their perceived stress and non-stress locations. The path was labelled using the commonly perceived stress and non-stress reported by the participants, as shown in Fig.

4(a). The proportion of the perceived stress along the path is presented in Table 3. The participants perceived 32.26% of the path as non-stress, 67.74% of the path as stress, 29.20% of the path as low stress, and 38.54% of the path as high stress. Although there is somewhat commonality in the participants' perceived stress and non-stress, their responses could be a mixed up of stress due to spatial factors (e.g., spatial configuration), temporal factors (e.g., noise level and weather) or individual factors (e.g., health condition and previous experience). Therefore the perceived response is complemented with physiological response to minimise the impact of stress and non-stress due to random or personal factors and maximise the impact of stress and non-stress due to spatial factors.

Table 3. Perceived stress distribution on the path.

| Segment | Total distance (m) | Non-stress (m) | Stress (m) | Low stress (m) | High stress (m) |
|---|---|---|---|---|---|
| A | 85.65 | 0 | 85.65 | 43.01 | 42.64 |
| B | 72.60 | 72.60 | 0 | 0 | 0 |
| C | 100.77 | 0 | 100.77 | 49.76 | 51.01 |
| D | 15.45 | 0 | 15.45 | 15.45 | 0 |
| E | 68.47 | 0 | 68.47 | 0 | 68.47 |
| F | 78.48 | 0 | 78.48 | 57.98 | 20.50 |
| G | 127.87 | 111 | 16.87 | 0 | 16.87 |
| H | 19.88 | 0 | 19.88 | 0 | 19.88 |
| Total | 569.17 | 32.26%* | 67.74%* | 29.20%* | 38.54%* |

*Note.* * = Percentage of the total path; m = metre.

A Wilcoxon signed-rank test was conducted to ascertain the differences in their physiological responses to path segments perceived as stress and non-stress. It was observed that some participants (e.g., participant 4) experienced a statistically significantly ($p < .05$) higher physiological response to part segments perceived as stress (median = 1.987) than part segments perceived non-stress (median = 1.132). Whereas other participants (e.g., participant 10) experienced a statistically significantly ($p < .05$) lower physiological response to part segments

perceived as stress (median = 1.487) than part segments perceived non-stress (median = 1.929). Akin to previous studies (Chrisinger and King, 2018; Birenboim et al., 2019; Lee et al., 2020; Saitis and Kalimeri, 2021), this result shows that either high or low physiological response is indicative of stress and non-stress environmental condition. Hence locations on the path with clusters of high statistical significant physiological responses (hot spots) and clusters of low statistical significant physiological responses (cold spots) were determined using spatial clustering analysis, specifically hot spot analysis.

The collective physiological responses were georeferenced to the corresponding GPS positions (Latitude and Longitude) for the entire path. The threshold distance for conceptualisation the spatial relationships determines the scale of the analysis, and influences the spatial clustering analysis (Mitchel, 2005). To determine the appropriate threshold distance, the authors measured the spatial autocorrelation for a series of distances and inspected their corresponding z-scores. A statistically significant high z-scores indicate the distances where spatial processes promoting clustering are most pronounced (Mitchel, 2005). The highest z-score ($p < 0.01$) was obtained at 11 m. Using Getis-Ord Gi* statistics with the scale of analysis set to 11 m, a hot spot analysis was conducted to determine the specific locations on the path that stimulated a common physiological reaction for the participants. The hot spot analysis result is presented in Fig. 4(b). A total of 1105 and 2178 sample points were determined as a hot spot and cold spot, respectively, at a 95% confidence level. In other words, these hot and cold spots were the results of older adults' physiological responses to spatial factors at a 95% confidence level. The 1105 and 2178 spatial significant sample points corresponding to the perceived responses were used to determine the stress and non-stress locations on the path in order to further analyse the spatial attributes—here,

the visuospatial configurations—stimulating such stress and non-stress responses. The hot spots and cold spots within the perceived stress path segments (i.e., 2161 points of spatial significant stress samples) were distributed approximately across seven locations on the path (i.e., S1 to S7) as shown in Fig. 4(c). The hot spots and cold spots within the perceived non-stress path segments (i.e., 1122 points of spatial significant stress samples) were distributed approximately across six locations on the path (i.e., N1 to N6) as shown in Fig. 4(d).
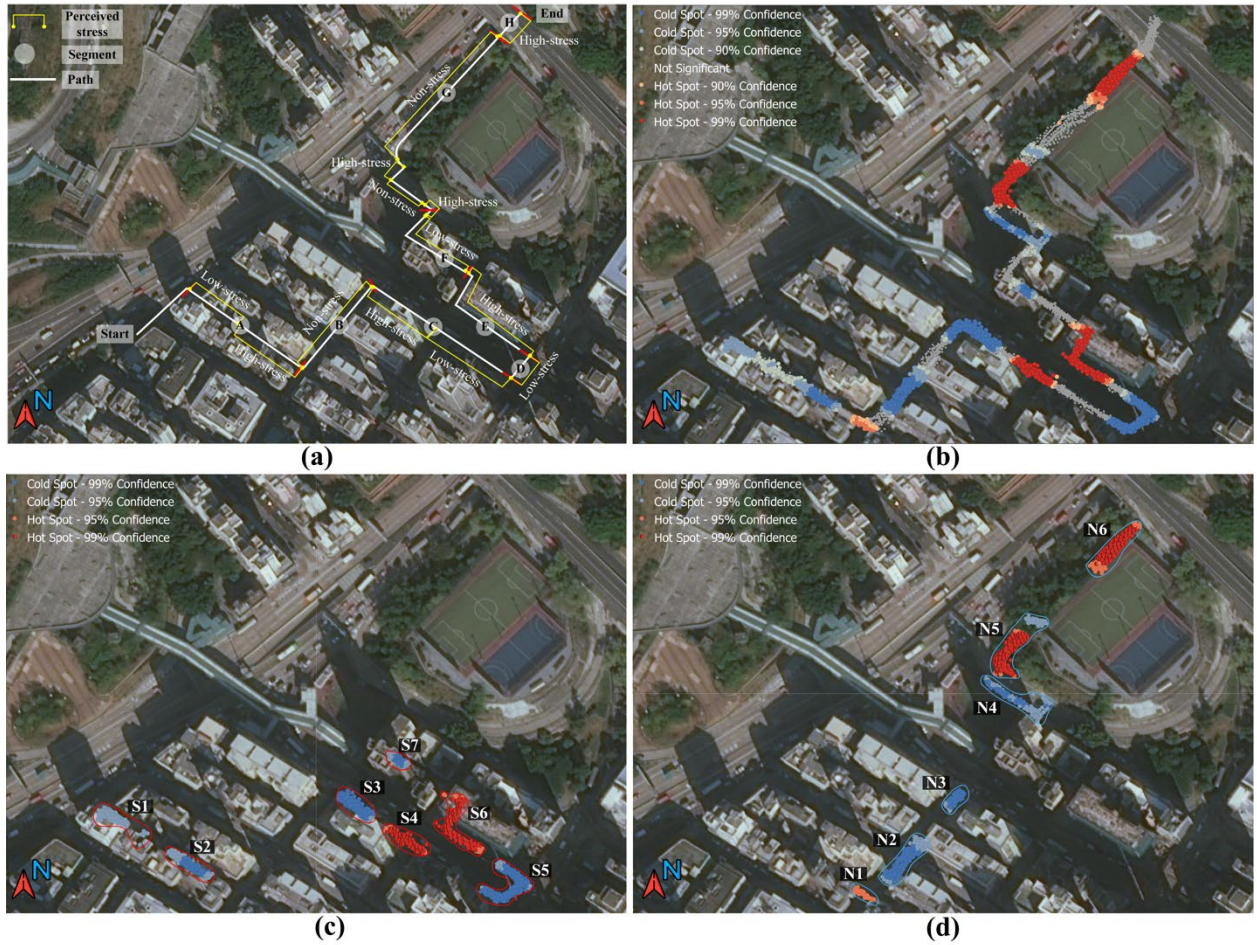


Fig. 4. (a) The commonly perceived stress and non-stress response by the participants. (b) Spatial significant clusters of high (hot spot) and low (cold spot) physiological responses of the participants. (c) The distribution of spatial significant stress locations on the path. S1 to S7 correspond to spatial significant stress locations based on physiological-perceived responses. (d) The distribution of spatial significant non-stress locations on the path. N1 to N6 correspond to non-stress locations based on physiological-perceived responses.

### 3.2. Influence of visuospatial perception on physiological response

Older adults' visuospatial perceptions (i.e., the values for all isovist indicators) were spatially matched with the spatial significant stress samples (2161 sample points) and non-stress samples (1122 sample points). A Wilcoxon signed-rank test was conducted to determine whether there is a significant difference in their visuospatial perceptions during stress and non-stress physiological states. The results indicate that all isovist indicators were statistically and significantly different under the two different physiological states with a 95% significance level. This is an indication that the isovist indicators somewhat influenced the participants' stress and non-stress physiological states.

Principal component analysis (PCA) was conducted on the spatially significant matched samples of isovist indicators and physiological responses for each field of view to determine whether the variation retained in the first two principal components contains relevant information about the samples. Before PCA was conducted, the data for each isovist indicator was mean centred and then divided by the standard deviation of the isovist indicator (data normalisation). This way, each isovist indicator has zero mean and unit standard deviation to ensure that the PCA is based on how much variation the isovist indicators explain to improve numerical stability. The biplots of the two largest principal components for 90° field of view, 120° field of view, and 180° field of view are shown in Fig. 5(a), Fig. 5(b), and Fig. 5(c), respectively. From the biplots, it can be observed that the two largest principal components (i.e., PC1 on the x-axis and PC2 on the y-axis) for all the fields of view explain more than 80% (i.e., the sum of PC1 and PC2) of the variability in the data. The biplot reveals that non-stress responses are characterised by increasing values of area, perimeter, occlusivity, minimum and maximum visibility, while stress is somewhat characterised

by increasing values of jaggedness and compactness. However, note that the PCA is only providing information on the global structure of the data; therefore, further data exploration was conducted using SOM and machine learning to understand the local structure of the data.



**(a)** PCA biplot: 90° field of view

**(b)** PCA biplot: 120° field of view

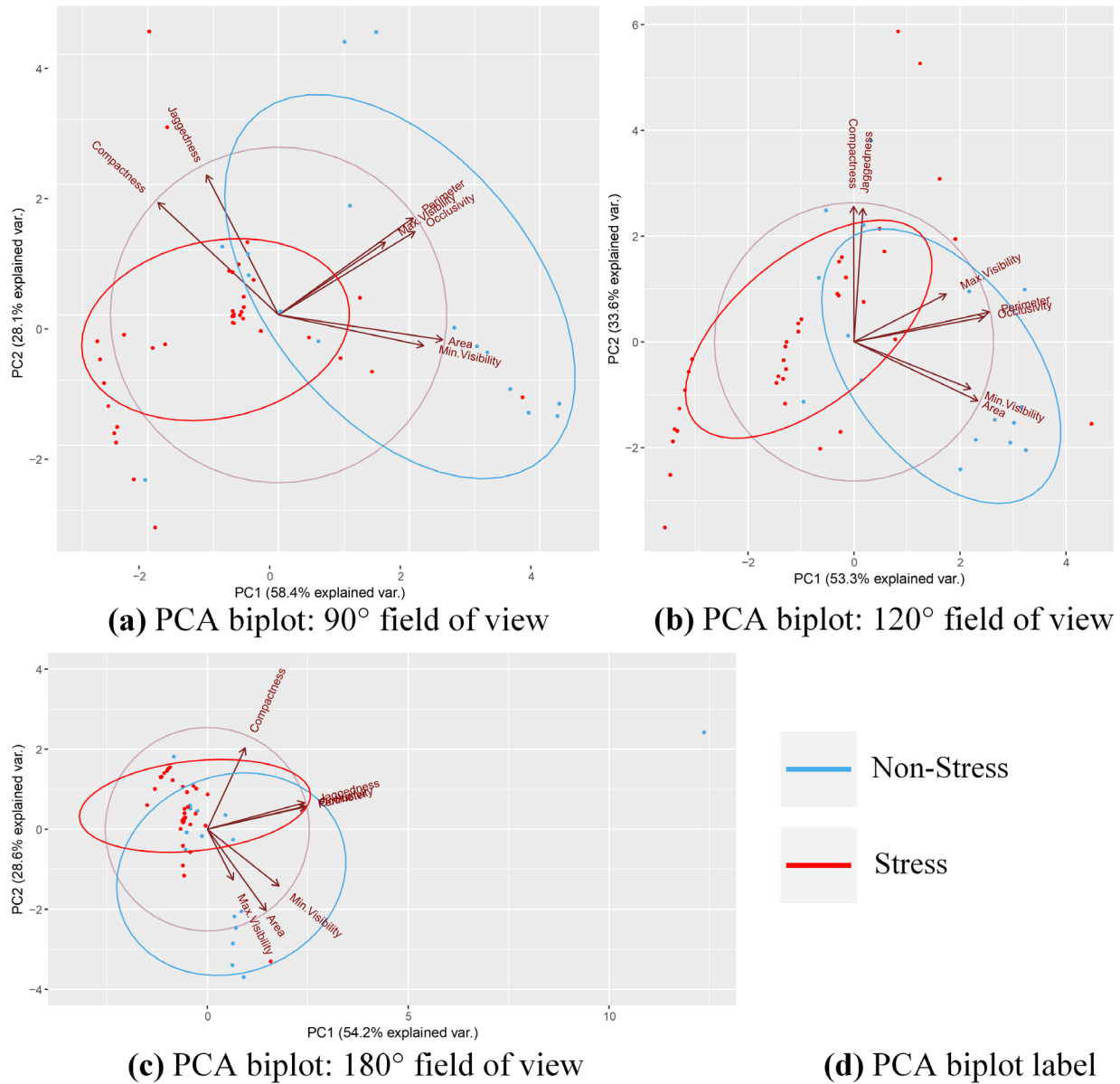**(c)** PCA biplot: 180° field of view

**(d)** PCA biplot label

Fig. 5. PCA biplot of spatially significant matched samples of isovist indicators and physiological responses. (a) 90° field of view. (b) 120° field of view. (c) 180° field of view. (d) PCA biplot label for stress and non-stress physiological responses. PC1 = principal component 1; PC2 = principal component 2.

The optimal hyperparameter settings for the SOM are reported in Table 4. Note that the isovist indicators were normalised. The learning process for 90° field of view, 120° field of view, and 180° field of view dataset are shown in Fig. 6(a), Fig. 6(d), and Fig. 6(g), respectively. Fig. 6(a), Fig. 6(d), and Fig. 6(g) show the mean distance to the closest unit decreased during the learning process, stabilised at a very small value and reached a minimum plateau. A small value of mean distance is an indication that the weight vector of a node is similar to the input data $x_i$ (isovist indicator) and corresponding label $y_i$ (physiological response) represented by that node. The marginal improvement in the mean distance after the first 60 iterations proves the convergence of the SOM. Fig. 6(b), Fig. 6(e), and Fig. 6(h) present the count plot for 90°, 120°, and 180° fields of view, respectively. The count plot shows the number of input data points in each node. The neighbourhood distance plots in Fig. 6(c), Fig. 6(f), and Fig. 6(i) for 90°, 120°, and 180° fields of view, respectively, shows further clustering in the data. Areas of low neighbour distance (dark regions) indicate the group of nodes with similar properties, and the further apart nodes (light regions) indicate natural borders in the map.

Hierarchical clustering analysis was conducted to show the clustering information in the SOM. The clustering shows a clear boundary of isovist indicators resulting in non-stress and stress physiological responses. The SOM with cluster boundaries for 90° field of view, 120° field of view, and 180° field of view analyses are presented in Fig. 7. The SOM shows the level of isovist indicators (Fig. 7[a], Fig. 7[d], and Fig. 7[g]) that influence older adults' physiological response (Fig. 7[b], Fig. 7[e], and Fig. 7[h]). The cluster of participants influence by a specific isovist indicator (s) is shown in Fig. 7(c), Fig. 7(f), and Fig. 7(i) for 90°, 120°, and 180° fields of view, respectively.

(a) Learning process: 90° field of view

(b) Count plot: 90° field of view

(c) Neighbour distance plot: 90° field of view

(d) Learning process: 120° field of view

(e) Count plot: 120° field of view

(f) Neighbour distance plot: 120° field of view

(g) Learning process: 180° field of view

(h) Count plot: 180° field of view
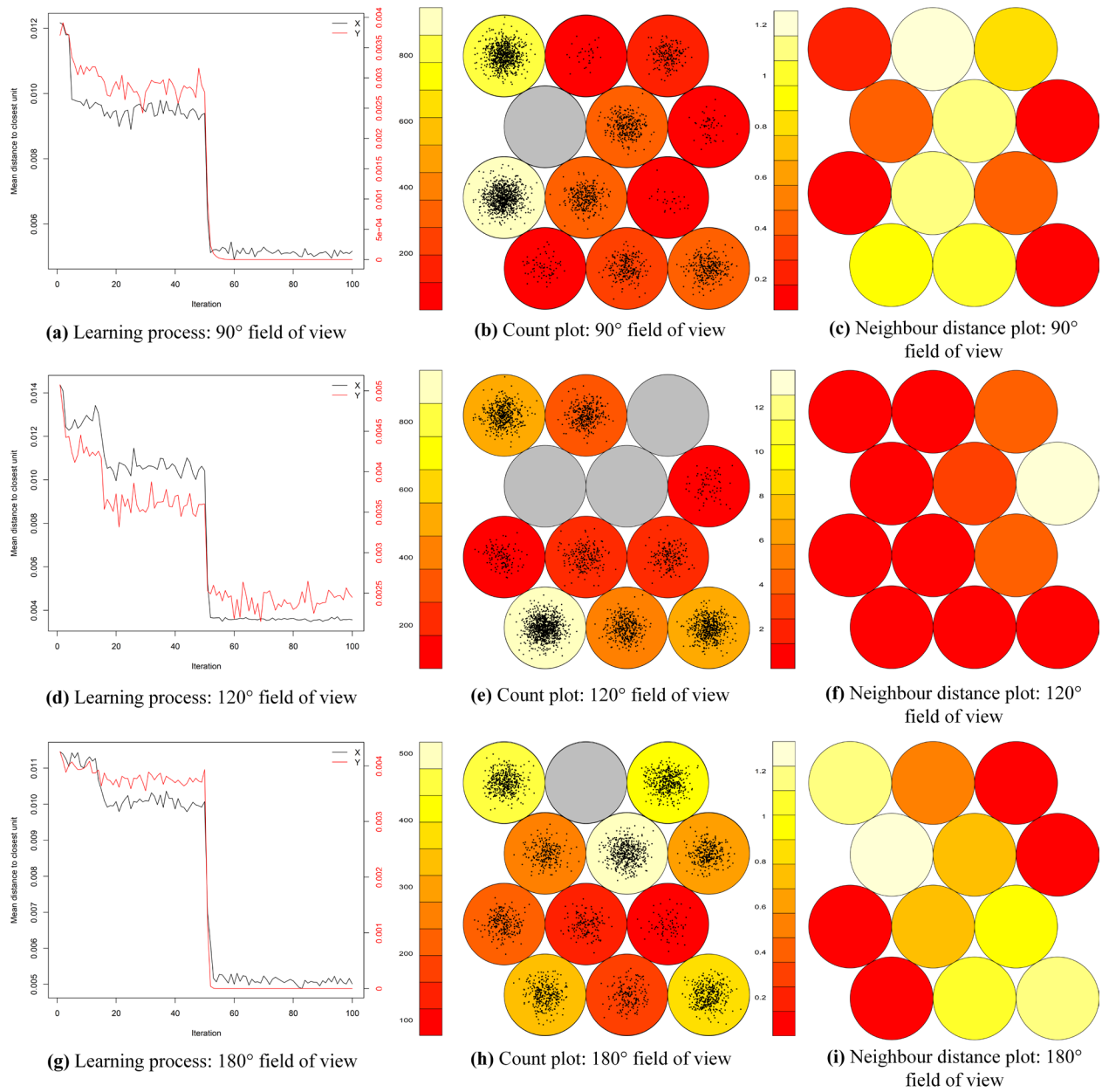
(i) Neighbour distance plot: 180° field of view

Fig. 6. SOM architecture.

32

Table 4. Optimal hyperparameters settings for SOM and SOM validation result.

| Hyperparameters | Field of view | | |
|---|---|---|---|
| | 90° | 120° | 180° |
| Grid size | 3×4 | 3×4 | 3×4 |
| Topography | Hexagonal | Hexagonal | Hexagonal |
| User weights | 0.8 | 0.2 | 0.8 |
| Distance weights | 2.444 | 2.444 | 2.444 |
| Neighbourhood function | Bubble | Bubble | Bubble |
| Distance function | Tanimoto | Tanimoto | Tanimoto |
| Training length | 100 | 100 | 100 |
| Learning rate (initial, final) | 0.05, 0.01 | 0.05, 0.01 | 0.05, 0.01 |
| 10-fold cross-validation | | | |
|   AUROC | 0.960 | 0.931 | 0.937 |
|   Sensitivity | 0.843 | 0.767 | 0.790 |
|   Specificity | 0.929 | 0.939 | 0.934 |

*Note.* AUROC = area under the receiver operating characteristic

The SOM reveals the local structure of the data. For instance, participant 1's experience is best captured by node 5, node 6, and node 9 for 90°, 120°, and 180° fields of view, respectively. Participant 1 experienced stress when there is a high level of maximum visibility, a medium level of compactness and low levels of area, minimum visibility, perimeter, occlusivity, and jaggedness for 90° and 180° fields of view. However, a small increase in minimum visibility and area resulted in a non-stress physiological response when the field of view is 120°. None of participant 8's data was captured in nodes 9 and 6 (90° fields of view), implying that the levels of isovist indicators in these nodes have no influence on participant 8. The male participants (participants 3, 5 and 10) samples dominated the count in node 1 (90° fields of view), indicating that minimum visibility, maximum visibility, area, perimeter and occlusivity (in order of importance) influence their physiological response.
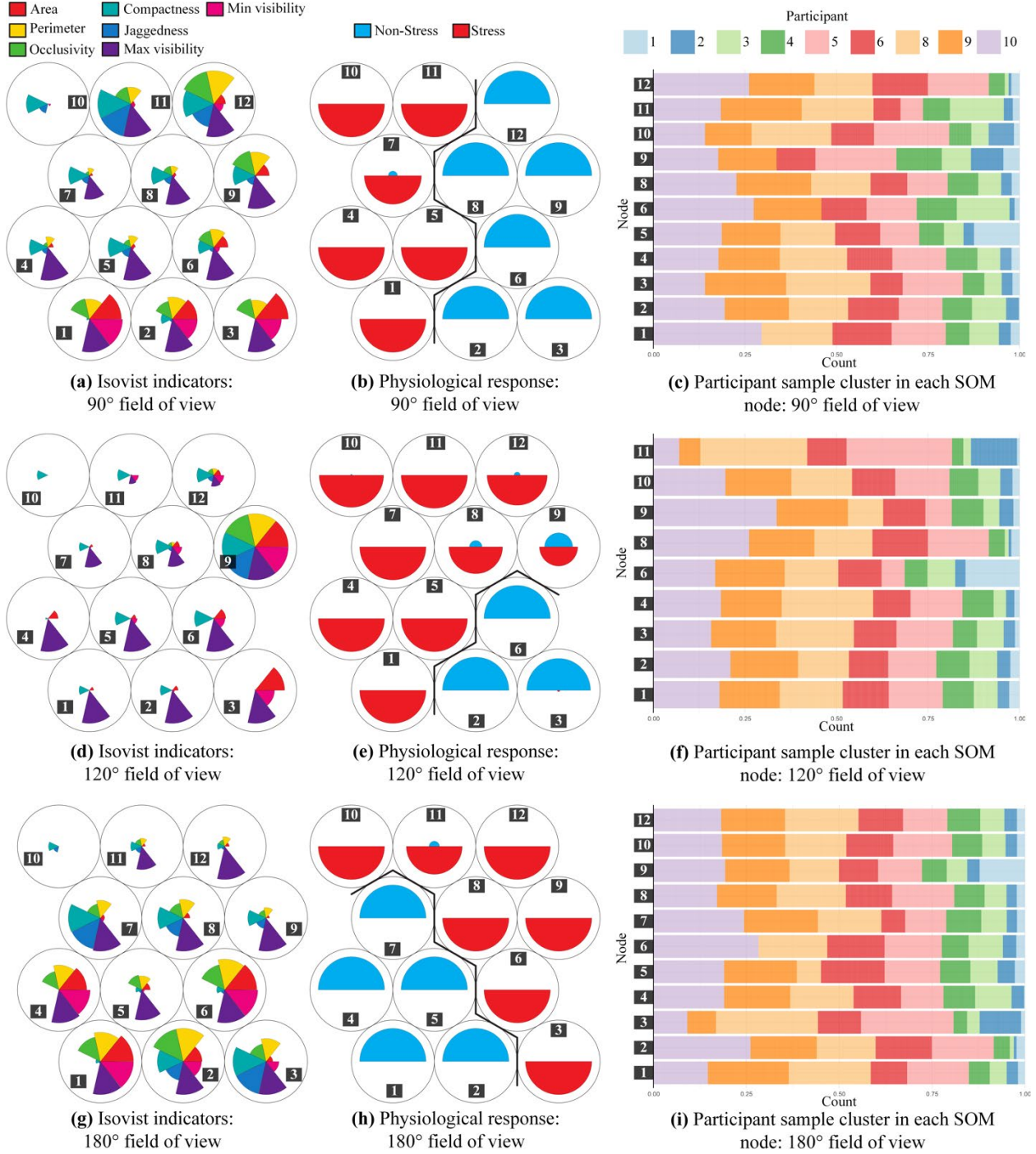
Fig. 7. Influence of isovist indicators on participants physiological stress. (a), (d), and (g) is a "fan diagram", each node of the "fan diagram" consist of individual fans, which represents the magnitude of each input variable (i.e., the isovist indicator) in the weight vector. (b), (e), and (h) is read in conjunction with (a). It shows the isovist indicator levels eliciting a specific physiological response. (c), (f), and (i) show the participants sample data that were clustered into a specific self-organising map (SOM) node. The SOM consist of 12 nodes.

### 3.3. Most influential isovist indicators of physiological response

The hierarchy of influential isovist indicator (s) subsets is provided in Fig. 8. Minimum visibility was the most influential under 90°, 120° and 180° fields of view. Most of the machine learning models achieved higher performance when only the most influential isovist indicator is used to discriminate between stress and non-stress physiological responses. Minimum visibility, occlusivity, perimeter, and isovist area (for 90° field of view); minimum visibility, occlusivity, isovist area, and compactness (for 120° field of view); and minimum visibility, isovist area, and occlusivity (for 180° field of view) appeared in most of the influential isovist indicator (s) subsets. The level of influence is presented alongside the dominant pattern observed in the PCA and SOM in Table 5.

**(a) Isovist indicator: 90° field of view**

| Hierarchy of influence | AUROC | | | | |
|---|---|---|---|---|---|
| | SVM | NB | LR | kNN | DT |
| MinV | 0.758 | 0.906 | 0.922 | 0.996 | 0.993 |
| MinV, O | 0.838 | 0.932 | 0.936 | 0.997 | 0.989 |
| MinV, O, P | 0.841 | 0.930 | 0.936 | 0.995 | 0.993 |
| MinV, O, P, A | 0.841 | 0.927 | 0.940 | 0.996 | 0.994 |
| MinV, O, P, A, MaxV | 0.838 | | 0.940 | 0.996 | |
| MinV, O, P, A, C, MaxV | 0.840 | 0.926 | 0.940 | 0.997 | 0.993 |
| MinV, O, P, A, C, MaxV, J | 0.841 | 0.924 | 0.944 | 0.996 | 0.991 |

**(b) Isovist indicator: 120° field of view**

| Hierarchy of influence | AUROC | | | | |
|---|---|---|---|---|---|
| | SVM | NB | LR | kNN | DT |
| MinV | 0.764 | 0.862 | 0.870 | 0.996 | 0.990 |
| MinV, O | 0.752 | 0.831 | | | 0.990 |
| MinV, O, A | 0.740 | 0.855 | 0.868 | | |
| MinV, O, A, C | 0.788 | 0.841 | 0.914 | 0.996 | |
| MinV, O, A, C, MaxV | 0.818 | 0.875 | | 0.996 | 0.991 |
| MinV, O, A, C, MaxV, P | 0.819 | 0.877 | 0.943 | 0.995 | 0.992 |
| MinV, O, A, C, MaxV, P, J | 0.819 | 0.872 | 0.952 | 0.996 | 0.992 |

**(c) Isovist indicator: 180° field of view**

| Hierarchy of influence | AUROC | | | | |
|---|---|---|---|---|---|
| | SVM | NB | LR | kNN | DT |
| MinV | 0.764 | 0.894 | 0.901 | 0.996 | 0.992 |
| MinV, A | 0.764 | 0.857 | 0.841 | 0.996 | 0.991 |
| MinV, A, O | 0.799 | 0.861 | 0.863 | 0.996 | 0.992 |
| MinV, A, O, P | | | 0.877 | | 0.990 |
| MinV, A, O, C, MaxV | | 0.858 | | 0.996 | 0.992 |
| MinV, A, O, C, MaxV, P | 0.802 | 0.859 | 0.904 | 0.997 | 0.993 |
| MinV, A, O, C, P, MaxV, J | 0.804 | 0.862 | 0.922 | 0.997 | 0.993 |

A – Isovist area
P – Isovist perimeter
O – Occlusivity
C – Compactness
J – Jaggedness
MaxV – Maximum visibility
MinV – Minimum visibility

DT – Decision tree:J48
kNN – k-nearest neighbour
LR – Logistic regression
NB – Naïve Bayes
SVM – Support vector machine
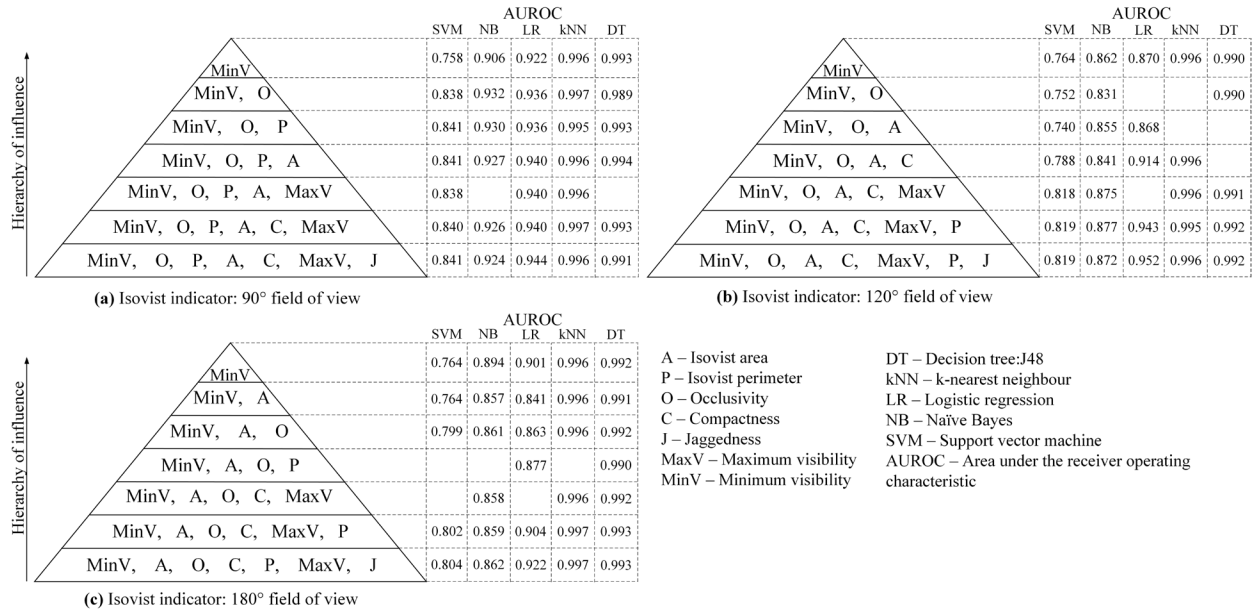AUROC – Area under the receiver operating characteristic

Fig. 8. Hierarchy of influential isovist indicator (s) subsets with corresponding performance when tested on machine learning algorithms with 10-fold cross-validation.

Table 5. Isovist indicators influence on physiological response

| Isovist indicator | 90° field of view | | 120° field of view | | 180° field of view | |
| --- | --- | --- | --- | --- | --- | --- |
| | Non-stress | Stress | Non-stress | Stress | Non-stress | Stress |
| Area | ↑4 | ↓4 | ↑3 | ↓3 | ↑2 | ↓2 |
| Perimeter | ↑3 | ↓3 | ↑6 | ↓6 | ↑4 | ↓4 |
| Occlusivity | ↑2 | ↓2 | ↑2 | ↓2 | ↑3 | ↓3 |
| Compactness | ↓6 | ↑6 | ↓4 | ↑4 | ↓4 | ↑4 |
| Jaggedness | ↓7 | ↑7 | ↓7 | ↑7 | ↓7 | ↑7 |
| Maximum visibility | ↑5 | ↓5 | ↑5 | ↓5 | ↑4 | ↓4 |
| Minimum visibility | ↑1 | ↓1 | ↑1 | ↓1 | ↑1 | ↓1 |

*Note.* ↑ = increase in isovist indicator; ↓ = decrease in isovist indicator; [1] = most influential; [7] = least influential.

## 4. Discussion

The result from the PCA, SOM, and machine learning algorithms show that minimum visibility, occlusivity, and isovist area have the most significant influence on physiological responses among older adults at individual and group levels. In the prospect-refuge theory, minimum visibility is the visual indicator for "refuge". This implies that older adults' physiological responses are strongly influenced in an environment with refuge value. Occlusivity is another indicator of refuge; occlusivity is the second most influential predictor of physiological response. However, when this refuge element is present, older adults displayed a preference for a high minimum visibility length and high occlusivity, which results in a non-stress response, while a low minimum visibility length and low occlusivity result in a stress response. Hong Kong has a high refuge value because its spatial configuration is enclosed by high-density and high-rise buildings. This explains why 'refuge' emerged as the most significant element in a visuospatial configuration. For older adults to experience a non-stress physiological response in a high refuge value environment such as Hong Kong, the spatial configuration should have more open edges (increased occlusivity) and a longer minimum nearest distance to physical boundaries (increased minimum visibility). This finding is quite interesting because it does not conform to the refuge theory (enclosure evokes a sense of

safety) because having more open edges and visibility increases the chances of being seen by other people. It is plausible that these isovist indicators (i.e., minimum visibility and occlusivity) captured the claustrophobic element in older adults' reaction, where a visuospatial configuration that is too enclosed triggers claustrophobic tendencies, causing an increase in physiological stress.

While the claustrophobic tendency explains the reason for such a physiological response, there might actually be more to it than that. A spatial configuration with more open edges (high occlusivity) tends to promise more information (mystery). Older adults are even more likely to experience non-stress physiological responses due to an increase in mystery when the field of view is between 90° and 180°. Therefore, creating a visuospatial configuration with high mystery might as well reduce the tendency of feeling claustrophobic among older adults.

Isovist area is another influential determinant of physiological response; its influence increases with an increasing field of view. The behavioural and experience relevance of the isovist area corresponds to "prospect" in the prospect-refuge theory. The perimeter and maximum visibility length also quantify the prospect theory. Older adults experienced a non-stress physiological response when the environment offers a configuration conducive to attaining a larger view, while a physiological stress response is experienced when the view is small. According to the prospect theory, being able to "fetch" information from all spaces at an observation point in a large space induces a sense of security. This explains why older adults experienced a non-stress physiological response when prospect elements (isovist area, perimeter, and maximum visibility length) increase.

Isovist area, compactness and maximum visibility became increasingly influential when the field of view increases. This could be because the distribution of visuospatial information increases with an increasing field of view. The complexity and mystery in the environment become more relevant when the field of view increases which can either cause humans to display preference or aversion depending on the varying proportions of the elements in the spatial configuration. Specifically, older adults experienced physiological stress when spatial complexity increases (i.e., increased compactness); this physiological stress due to complexity is even more likely when the field of view increases. A more critical look into the local structure of the data in the SOM shows that weakness in any specific quality (e.g., lack of prospect elements due to layout restrictions) can be compensated for with the strength in others (e.g., increasing the value of mystery) when designing spatial layouts that stimulate a specific physiological effect.

## 4.1. Comparison with similar studies

Previous researchers (as shown in Table 6) that have studied this topic mainly focused on younger adults with an average age of about 25 years. These studies were conducted in Switzerland, Germany and Hong Kong. Interestingly, there are some differences and commonalities between the impact of visuospatial configurations on younger adults and older adults.

Study 1 and Study 5 finds that younger adults prefer urban spaces that are enclosed in order for them to feel safe. These findings on younger adults are contrary to the current finding on older adults; older adults feel claustrophobic (leading to physiological stress) when the urban spaces are too enclosed or when they are too close to a physical boundary (e.g., a wall). Older adults show a preference for spaces that are not too enclosed with more open edges in order for them to be seen

by other pedestrians. Study 3 and Study 4 reports that younger adults perceived spaces with high visibility and perimeter to be stressful because they can be seen from a larger area. In contrast, older adults experienced a non-stress physiological response when urban spaces have a larger view and perimeter because they are able to see all their surroundings which heighten the feeling of security. In summary, older adults prefer urban spaces where they can be seen, while younger adults prefer spaces where they cannot be seen.

While Study 1 and Study 2 conclude that higher compactness causes positive emotions for younger adults, this current study indicates that higher compactness causes physiological stress for older adults. The results from Study 3 shows that younger adults are more likely to perceive an urban space with low complexity (measured using isovist vertices numbers) as stressful. However, Study 5 presented that high complexity (measured using jaggedness) is related to younger adults' negative emotions. In this current study, older adults felt stressed when complexity (measured using jaggedness) increases.

While these differences are worth sharing, theoretically, it should be noted that the spatial layout, living arrangement, and cultural background in these countries are different, which can influence an individual's response. Methodologically, all these studies, including the presented study, were limited to two dimensional isovist which omits other relevant spatial factors. Study 1, 2, 4 and 5 used only physiological responses for their analysis and Study 3 used only perceived responses for their analysis. This study combined both perceived and physiological responses.

Table 6. Summary of previous studies.

| Study | Background | Visuospatial element | Influence |
|---|---|---|---|
| Study 1: Li et al. (2016) | Participants' mean age: 25 (2.5 standard deviation) Experiment location: Zürich, Switzerland Data: Skin conductivity | Compactness | Higher compactness causes positive emotion |
| | | Maximum visibility | Higher visibility causes positive emotion |
| | | Refuge value (minimum visibility or occlusivity) | Enclosed urban spaces are very important in fostering a sense of security in pedestrians |
| Study 2: Hijazi et al. (2016) | Participants: Students and lecturers Experiment location: Zürich, Switzerland Data: Skin conductivity | Occlusivity (60°) | Significant for predicting negative emotional arousal |
| | | Perimeter (360°) | Significant for predicting negative emotional arousal |
| | | Compactness (360°) | Significant for predicting positive emotional arousal |
| | | Perimeter (60°) | Significant for predicting positive emotional arousal |
| | | Occlusivity (60°) | Significant for predicting positive emotional arousal |
| Study 3: Knöll et al. (2018) | Participants' median age: 25 years (range 22 to 35, 2.2 standard deviation) Experiment location: Darmstadt, Germany Data: Questionnaire to collect perceived urban stress | Visibility | Visibility is positively related to perceived urban stress |
| | | Perimeter | Perimeter is positively related to perceived urban stress |
| | | Isovist vertices numbers (indicates the complexity) | Isovist vertices numbers relate negatively to perceived urban stress |
| | | Visibility and perimeter Vertices number | Outdoor spaces visibility and perimeter, which describe the shape of space and vertices number, which indicates the complexity of a shape, are more important isovist characteristics to explain perceived urban stress. |
| Study 4: Ojha et al. (2019) | Participants' mean age: Not provided Experiment location: Zürich, Switzerland Data: Skin conductivity | Isovist area | High value of isovist area resulted in an aroused physiological state |
| | | Perimeter | Data was collected, but result was not reported |
| | | Compactness | Data was collected, but the result was not reported |
| | | Occlusivity | Data was collected, but the result was not reported |
| | | Isovist area (90°) | Negatively related to negative emotion |

| Study | Background | Visuospatial element | Influence |
|---|---|---|---|
| Study 5: Xiang et al. (2020) | Participants' mean age: 24.77 years (0.718 standard deviation) Experiment location: Hong Kong Data: Skin conductivity | Compactness | Insignificant |
| | | Isovist drift angle (90°) | Negatively related to negative emotion |
| | | Isovist drift magnitude (90°, 120°, 180°) | Negatively related to negative emotion |
| | | Max-radial (90°, 120°) | Negatively related to negative emotion |
| | | Occlusivity | Insignificant |
| | | Perimeter (90°, 120°) | Negatively related to negative emotion |
| | | Jaggedness (90°, 120°, 180°) | Positively related to negative emotion |
| | | Enclosure (refuge value) | To avoid negative emotions, the space must be enclosed to guarantee a sense of security |

## 4.2. Limitations and future direction

This study is not without limitations. The number of participants is relatively small, the data was collected on a predefined path (the path was subjectively selected), and the environmental walk lasted for a few days. The above limitations could affect the generalisation of the results. Limiting the path choice for older adults could affect how they interacted with the environment; in the real world, people usually have the option to decide what path to use. The above conditions were necessary to appropriately collect and match the visual perception data with the physiological response. Future data collection will be conducted in an elderly community where the paths are not so restricted. The collection of physiological responses (i.e., the first phase of the environmental walk) and perceived responses (i.e., the second phase of the environmental walk) were not concurrent, and post-rationalisation may have occurred. Future studies should consider synchronising both physiological and perceived stress data collection. For example, the participants can document their perceived responses with an elderly-friendly mobile application

while wearing a wristband-band type sensor. The physiological-perceived stress detection method in this study only reduced the effect of the temporal and individual factors, which means there is still a possibility that these factors influenced their stress and non-stress responses. Also, additional spatial attributes such as three-dimensional isovist, building surface characteristics and appearance (e.g., material, texture, and colour), and several urban metrics were not considered in the analysis but could influence stress responses. More complex issues such as what the participants actually see and whether they have any visual impairments need further deliberation to understand the influence of visuospatial properties on stress. It should be mention that a wearable electroencephalography (EEG) headset and an insole foot plantar pressure sensor were used during the data collection, but the results from these sensors were not informative enough, hence not considered in this study.

Further research is being conducted to understand the influence of surface characteristics and appearance (e.g., material, texture, and colour) on older adults' physiological stress. The generative potential of the multi-objective evolutionary algorithm will be exploited to generate geometrical designs with specific physiological effects that can fit into new or existing spaces in the urban environment.

## 5. Conclusions

This study aimed to understand the influence of visuospatial configurations of urban space on older adults' physiological stress. Older adults' physiological response (PPG) and perceived stress responses were analysed using spatial clustering hot spot analysis to detect stressful person-environment interactions due to spatial factors. Two-dimensional isovist analysis was used to used

quantify older adults visuospatial perception of the urban environment. The influence of urban visuospatial configurations on stress was established using principal component analysis, self-organising maps and machine learning algorithms. The following conclusions were made. (1) Isovist minimum visibility, occlusivity, and isovist area are the most influential determinants of older adults' physiological response. (2) Older adults experienced a non-stress physiological response when prospect elements (isovist area, perimeter, and maximum visibility length) increase. (3) Older adults feel stressed when the environment is too enclosed. (4) Isovist indicators can complement one another to achieve a specific physiological effect. (5) Older adults prefer urban configurations where they can be seen. Overall, the findings from this study can be used to inform urban design and planning.

## References

Acharya, U. R., Joseph, K. P., Kannathal, N., Lim, C. M., & Suri, J. S. (2006). Heart rate variability: A review. *Medical and Biological Engineering and Computing*, *44*(12), 1031-1051. https://doi.org/10.1007/s11517-006-0119-0

Appleton, J. (1975). *The Experience of Landscape*. John Wiley and Sons, London.

Banaei, M., Hatami, J., Yazdanfar, A., & Gramann, K. (2017). Walking through architectural spaces: the impact of interior forms on human brain dynamics. *Frontiers in Human Neuroscience*, *11*, 477. https://doi.org/10.3389/fnhum.2017.00477

Barrett, L. F., & Russell, J. A. (1998). Independence and bipolarity in the structure of current affect. *Journal of Personality and Social Psychology*, *74*(4), 967. https://doi.org/10.1037/0022-3514.74.4.967

Batty, M. (2001). Exploring isovist fields: Space and shape in architectural and urban morphology. *Environment and Planning B: Planning and Design*, *28*(1), 123-150. https://doi.org/10.1068/b2725

Benedikt, M. L. (1979). To take hold of space: Isovists and isovist fields. *Environment and Planning B: Planning and Design*, *6*(1), 47-65. https://doi.org/10.1068/b060047

Bengio, Y., & Grandvalet, Y. (2004). No unbiased estimator of the variance of k-fold cross-validation. *Journal of Machine Learning Research*, *5*(1532-4435), 1089–1105. https://doi.org/1089-1105. 10.5555/1005332.1044695

Birenboim, A., Dijst, M., Scheepers, F. E., Poelman, M. P., & Helbich, M. (2019). Wearables and location tracking technologies for mental-state sensing in outdoor environments. *The Professional Geographer*, *71*(3), 449-461. https://doi.org/10.1080/00330124.2018.1547978

Brown, C. D., & Davis, H. T. (2006). Receiver operating characteristics curves and related decision measures: A tutorial. *Chemometrics and Intelligent Laboratory Systems*, *80*(1), 24-38. https://doi.org/10.1016/j.chemolab.2005.05.004

Çekmiş, A., Hacıhasanoğlu, I., & Ostwald, M. J. (2014). A computational model for accommodating spatial uncertainty: Predicting inhabitation patterns in open-planned spaces. *Building and Environment*, *73*, 115-126. https://doi.org/10.1016/j.buildenv.2013.11.023

Charlton, P. H., Celka, P., Farukh, B., Chowienczyk, P., & Alastruey, J. (2018). Assessing mental stress from the photoplethysmogram: A numerical study. *Physiological Measurement*, *39*(5), 054001. https://doi.org/10.1088/1361-6579/aabe6a

Chemero, A. (2003). An outline of a theory of affordances. *Ecological Psychology*, *15*(2), 181-195. https://doi.org/10.1207/S15326969ECO1502_5

Chiu, H. F. K., Lam, L. C. W., Chi, I., Leung, T., Li, S. W., Law, W. T., Chung, D.W.S., Fung, H. H. L., Kan, P. S., Lum, C. M., Ng, J., & Lau, J. (1998). Prevalence of dementia in Chinese elderly in Hong Kong. *Neurology*, *50*(4), 1002-1009. https://doi.org/10.1212/WNL.50.4.1002

Chrisinger, B. W., & King, A. C. (2018). Stress experiences in neighborhood and social environments (SENSE): A pilot study to integrate the quantified self with citizen science to improve the built environment and health. *International Journal of Health Geographics*, *17*(1), 17. https://doi.org/10.1186/s12942-018-0140-1

Chun, J. A., Psarras, S., & Koutsolampros, P. (2019). Agent based simulation for 'Choice of Seats': A Study on the Human Space Usage Pattern. In *Proceedings of the 12th International Space Syntax Symposium. International Space Syntax Symposium*. Beijing, China. https://discovery.ucl.ac.uk/id/eprint/10072241

Dagnelie, G. (2011). *Visual prosthetics: physiology, bioengineering, rehabilitation*. Springer Science & Business Media.

Dawes, M. J., & Ostwald, M. J. (2013). Using isovists to analyse Prospect-Refuge Theory: Measuring Spatio-Visual Relations in Wright's Heurtley House. *The International Journal of the Constructed Environment*, *1*(3), 25-40.

Dawes, M. J., & Ostwald, M. J. (2014). Prospect-Refuge theory and the textile-block houses of Frank Lloyd Wright: An analysis of spatio-visual characteristics using isovists. *Building and Environment*, *80*, 228-240. https://doi.org/10.1016/j.buildenv.2014.05.026

Empatica (2020). *E4 data-BVP expected signal.* Available at https://support.empatica.com/hc/en-us/articles/360029719792-E4-data-BVP-expected-signal (accessed 6 November 2020).

Ergan, S., Radwan, A., Zou, Z., Tseng, H. A., & Han, X. (2019). Quantifying human experience in architectural spaces with integrated virtual reality and body sensor networks. *Journal of Computing in Civil Engineering*, *33*(2), 04018062. https://doi.org/10.1061/(ASCE)CP.1943-5487.0000812

Franz, G., & Wiener, J. M. (2005). Exploring isovist-based correlates of spatial behavior and experience. In van Nes, A. (Ed.) *5th International Space Syntax Symposium* (pp. 503-517). Techne Press, Amsterdam, The Netherlands. http://hdl.handle.net/11858/00-001M-0000-0013-D55F-8

Gehl, J. (2011). *Life between buildings: Using public space*. Island press.

Gibson, J. J. (1977). The theory of affordances. *Hilldale, USA*, *1*(2), 67-82.

Giseop, K. I. M., Ayoung, K. I. M., & Youngchul, K. I. M. (2019). A new 3D space syntax metric based on 3D isovist capture in urban space using remote sensing technology. *Computers, Environment and Urban Systems*, *74*, 74-87. https://doi.org/10.1016/j.compenvurbsys.2018.11.009

Hagedorn, R. (2001). *Foundations for practice in occupational therapy*. Elsevier, Edinburgh, UK.

Hall, M. A. (1999). *Correlation-based feature selection for machine learning* [Doctoral dissertation, Department of Computer Science, Waikato University, New Zealand]. https://www.cs.waikato.ac.nz/~ml/publications/1999/99MH-Thesis.pdf

Healey, J. A., & Picard, R. W. (2005). Detecting stress during real-world driving tasks using physiological sensors. *IEEE Transactions on Intelligent Transportation Systems*, *6*(2), 156-166. https://doi.org/10.1109/TITS.2005.848368

Heo, S., Kwon, S., & Lee, J. (2021). Stress detection with single PPG sensor by orchestrating multiple denoising and peak-detecting methods. *IEEE Access*, *9*, 47777-47785. https://doi.org/10.1109/ACCESS.2021.3060441

Hijazi, I. H., Koenig, R., Schneider, S., Li, X., Bielik, M., Schmit, G. N. J., & Donath, D. (2016). Geostatistical analysis for the study of relationships between the emotional responses of urban walkers to urban spaces. *International Journal of E-Planning Research (IJEPR)*, *5*(1), 1-19. https://doi.org/10.4018/IJEPR.2016010101

James, G., Witten, D., Hastie, T., & Tibshirani, R. (2013). *An introduction to statistical learning* (Vol. 112, p. 18). Springer, New York. https://doi.org/10.1007/978-1-4614-7138-7

Kabisch, N., Püffel, C., Masztalerz, O., Hemmerling, J., & Kraemer, R. (2021). Physiological and psychological effects of visits to different urban green and street environments in older people: A field experiment in a dense inner-city area. *Landscape and Urban Planning*, *207*, 103998. https://doi.org/10.1016/j.landurbplan.2020.103998

Kalache, A., & Kickbusch, I. (1997). A global strategy for healthy ageing. *World Health*, *50*(4), 4-5. https://apps.who.int/iris/bitstream/handle/10665/330616/WH-1997-Jul-Aug-p4-5-eng.pdf

Kaplan, S. (1988). Perception and landscape: Conceptions and misconceptions. In *(Ed. Nasar, J.) Environmental aesthetics: Theory, research, and application*.

Kiefer, P., Giannopoulos, I., Raubal, M., & Duchowski, A. (2017). Eye tracking for spatial research: Cognition, computation, challenges. *Spatial Cognition & Computation*, *17*(1-2), 1-19. https://doi.org/10.1080/13875868.2016.1254634

Kim, J., Ahn, C. R., & Nam, Y. (2019). The influence of built environment features on crowdsourced physiological responses of pedestrians in neighborhoods. *Computers, Environment and Urban Systems*, *75*, 161-169. https://doi.org/10.1016/j.compenvurbsys.2019.02.003

Knöll, M., Neuheuser, K., Cleff, T., & Rudolph-Cleff, A. (2018). A tool to predict perceived urban stress in open public spaces. *Environment and Planning B: Urban Analytics and City Science*, *45*(4), 797-813. https://doi.org/10.1177/0265813516686971

Kogler, L., Müller, V. I., Chang, A., Eickhoff, S. B., Fox, P. T., Gur, R. C., & Derntl, B. (2015). Psychosocial versus physiological stress—Meta-analyses on deactivations and activations of the

neural correlates of stress reactions. *Neuroimage*, *119*, 235-251. https://doi.org/10.1016/j.neuroimage.2015.06.059

Kohonen, T. (2013). Essentials of the self-organizing map. *Neural Networks*, *37*, 52-65. https://doi.org/10.1016/j.neunet.2012.09.018

Kuzmanovski, I., Dimitrovska-Lazova, S., & Aleksovska, S. (2007). Classification of perovskites with supervised self-organizing maps. *Analytica Chimica Acta*, *595*(1-2), 182-189. https://doi.org/10.1016/j.aca.2007.04.062

Lao, S. S. W., Low, L. P. L., & Wong, K. K. Y. (2019). Older residents' residents' perceptions of family involvement in residential care. *International Journal of Qualitative Studies on Health and Well-Being*, *14*(1), 1611298. https://doi.org/10.1080/17482631.2019.1611298

Lawton, M. P. (1982). Competence, environmental press, and the adaptation of older people. *Aging and the Environment: Theoretical Approaches*, 33-59.

Lazarus, R. S. (1990). Theory-based stress measurement. *Psychological Inquiry*, *1*(1), 3-13. https://doi.org/10.1207/s15327965pli0101_1

Lee, G., Choi, B., Ahn, C. R., & Lee, S. (2020). Wearable biosensor and hotspot analysis–based framework to detect stress hotspots for advancing elderly's mobility. *Journal of Management in Engineering*, *36*(3), 04020010. https://doi.org/10.1061/(ASCE)ME.1943-5479.0000753

Li, X., Hijazi, I., Koenig, R., Lv, Z., Zhong, C., & Schmitt, G. (2016). Assessing essential qualities of urban space with emotional and visual data based on GIS technique. *ISPRS International Journal of Geo-Information*, *5*(11), 218. https://doi.org/10.3390/ijgi5110218

Ma, L., Zhang, H., & Lu, M. (2020). Building's fractal dimension trend and its application in visual complexity map. *Building and Environment*, *178*, 106925. https://doi.org/10.1016/j.buildenv.2020.106925

Mair, C. A., Cutchin, M. P., & Peek, M. K. (2011). Allostatic load in an environmental riskscape: The role of stressors and gender. *Health & Place*, *17*(4), 978-987. https://doi.org/10.1016/j.healthplace.2011.03.009

Meilinger, T., Franz, G., & Bülthoff, H. H. (2012). From isovists via mental representations to behaviour: first steps toward closing the causal chain. *Environment and Planning B: Planning and Design*, *39*(1), 48-62. https://doi.org/10.1068/b34048t

Mitchel, A. (2005). *The ESRI Guide to GIS analysis, Volume 2: Spatial measurements and statistics.* ESRI Press.

Ojha, V. K., Griego, D., Kuliga, S., Bielik, M., Buš, P., Schaeben, C., Treyer, L., Standfest, M., Schneider, S., König, R., & Donath, D. (2019). Machine learning approaches to understand the influence of urban environments on human's physiological response. *Information Sciences, 474*, 154-169. https://doi.org/10.1016/j.ins.2018.09.061

OpenStreetMap and Contributors (2019). Planet dump retrieved from https://planet.osm.org, Available at: https://www.openstreetmap.org (accessed 11 November 2019).

Ord, J. K., & Getis, A. (1995). Local spatial autocorrelation statistics: distributional issues and an application. *Geographical Analysis*, *27*(4), 286-306. https://doi.org/10.1111/j.1538-4632.1995.tb00912.x

Ostwald, M. J., & Dawes, M. (2013). Prospect-refuge patterns in Frank Lloyd Wright's Prairie houses: Using isovist fields to examine the evidence. *The Journal of Space Syntax*, *4*(1), 136-159.

Panicker, S. S., & Gayathri, P. (2019). A survey of machine learning techniques in physiology based mental stress detection systems. *Biocybernetics and Biomedical Engineering*, *39*(2), 444-469. https://doi.org/10.1016/j.bbe.2019.01.004

Platon, L., Zehraoui, F., & Tahi, F. (2017). Self-organizing maps with supervised layer. In *2017 12th International Workshop on Self-Organizing Maps and Learning Vector Quantization, Clustering and Data Visualization (WSOM)* (pp. 1-8). IEEE. https://doi.org/10.1109/WSOM.2017.8020022

Portegijs, E., Rantakokko, M., Viljanen, A., Rantanen, T., & Iwarsson, S. (2017). Perceived and objective entrance-related environmental barriers and daily out-of-home mobility in community-dwelling older people. *Archives of Gerontology and Geriatrics*, *69*, 69-76. https://doi.org/10.1016/j.archger.2016.11.011

Rantanen, T. (2013). Promoting mobility in older people. *Journal of Preventive Medicine and Public Health*, *46*(Suppl 1), S50. https://doi.org/10.3961/jpmph.2013.46.S.S50

Resende, M. G., & Ribeiro, C. C. (2010). Greedy randomized adaptive search procedures: Advances, hybridizations, and applications. In *Gendreau M., Potvin J. Y. (eds) Handbook of Metaheuristics* (pp. 283-319). Springer, Boston, MA. https://doi.org/10.1007/978-1-4419-1665-5_10

Reynald, D. M., & Elffers, H. (2009). The future of Newman's Defensible Space Theory: Linking Defensible Space and the routine activities of place. *European Journal of Criminology*, *6*(1), 25-46. https://doi.org/10.1177/1477370808098103

Rishi, P., & Khuntia, G. (2012). Urban environmental stress and behavioral adaptation in Bhopal City of India. *Urban Studies Research*, *2012*, 635061. https://doi.org/10.1155/2012/635061

Saitis, C., & Kalimeri, K. (2021). Multimodal classification of stressful environments in visually impaired mobility using EEG and peripheral biosignals. *IEEE Transactions on Affective Computing*, *12*(1), 203-214. https://doi.org/10.1109/TAFFC.2018.2866865

Scherer, K. R. (2005). What are emotions? And how can they be measured? *Social Science Information*, *44*(4), 695-729. https://doi.org/10.1177/0539018405058216

Schneider, S., & Koenig, R. (2012). Exploring the generative potential of isovist fields: The evolutionary generation of urban layouts based on isovist field properties. In *30th International Conference on Education Research in Computer Aided Architectural Design in Europe, Prague* (pp. 355–363).

Scott, S. C. (1993). Complexity and mystery as predictors of interior preferences. *Journal of Interior Design*, *19*(1), 25-33. https://doi.org/10.1111/j.1939-1668.1993.tb00149.x

Shaffer, F., & Ginsberg, J. P. (2017). An overview of heart rate variability metrics and norms. *Frontiers in Public Health*, *5*, 258. https://doi.org/10.3389/fpubh.2017.00258

Shemesh, A., Talmon, R., Karp, O., Amir, I., Bar, M., & Grobman, Y. J. (2017). Affective response to architecture–investigating human reaction to spaces with different geometry. *Architectural Science Review*, *60*(2), 116-125. https://doi.org/10.1080/00038628.2016.1266597

Shumway-Cook, A., Patla, A., Stewart, A., Ferrucci, L., Ciol, M. A., & Guralnik, J. M. (2003). Environmental components of mobility disability in community-living older persons. *Journal of*

*the American Geriatrics Society*, *51*(3), 393-398. https://doi.org/10.1046/j.1532-5415.2003.51114.x

SpaceGroupUCL (2019). DepthmapX Multi-Platform Spatial Network Analysis Software. Version 0.7.0 Open Source. Available at: https://github.com/SpaceGroupUCL/depthmapX/releases/tag/v0.7.0 (accessed 3 July 2020).

Szinte, M., & Cavanagh, P. (2012). Apparent motion from outside the visual field, retinotopic cortices may register extra-retinal positions. *PLoS One 7*(10), e47386. https://doi.org/10.1371/journal.pone.0047386

Tarvainen, M. P., Niskanen, J. P., Lipponen, J. A., Ranta-Aho, P. O., & Karjalainen, P. A. (2014). Kubios HRV–heart rate variability analysis software. *Computer Methods and Programs in Biomedicine*, *113*(1), 210-220. https://doi.org/10.1016/j.cmpb.2013.07.024

Torku, A., Chan, A. P. C., & Yung, E. H. K. (2020). Age-friendly cities and communities: A review and future directions. *Ageing & Society*, 1-38. https://doi.org/10.1017/S0144686X20000239

Turner, A., Doxa, M., O'sullivan, D., & Penn, A. (2001). From isovists to visibility graphs: A methodology for the analysis of architectural space. *Environment and Planning B: Planning and Design*, *28*(1), 103-121. https://doi.org/10.1068/b2684

United Nations (2020). *World Population Ageing 2020 Highlights: Living arrangements of older persons*. United Nations, New York. ST/ESA/SER.A/451

van Heezik, Y., Freeman, C., Buttery, Y., & Waters, D. L. (2020). Factors affecting the extent and quality of nature engagement of older adults living in a range of home types. *Environment and Behavior*, *52*(8), 799-829. https://doi.org/10.1177/0013916518821148

Verbrugge, L. M. (2020). Revisiting the disablement process. In *Jagger C., Crimmins E., Saito Y., De Carvalho Yokota R., Van Oyen H., & Robine J. M. (eds) International Handbook of Health Expectancies* (pp. 275-285). Springer, Cham. https://doi.org/10.1007/978-3-030-37668-0_20

Verbrugge, L. M., & Jette, A. M. (1994). The disablement process. *Social Science & Medicine*, *38*(1), 1-14. https://doi.org/10.1016/0277-9536(94)90294-1

Vesanto, J., & Alhoniemi, E. (2000). Clustering of the self-organizing map. *IEEE Transactions on Neural Networks*, *11*(3), 586-600. https://doi.org/10.1109/72.846731

Webber, S. C., Porter, M. M., & Menec, V. H. (2010). Mobility in older adults: A comprehensive framework. *The Gerontologist*, *50*(4), 443-450. https://doi.org/10.1093/geront/gnq013

WHO (World Health Organisation) (2001). *International classification of functioning, disability, and health.* WHO, Geneva, Switzerland.

WHO (World Health Organisation) (2007). *Global age-friendly cities: A guide*. WHO Press, Geneva.

WHO (World Health Organisation) (2018). *The Global Network for Age-friendly Cities and Communities: Looking back over the last decade, looking forward to the next*. WHO, Geneva, Switzerland.

Wiener, J. M., & Franz, G. (2004). Isovists as a means to predict spatial experience and behavior. In *International Conference on Spatial Cognition* (pp. 42-57). Springer, Berlin, Heidelberg. https://doi.org/10.1007/978-3-540-32255-9_3

Wongravee, K., Lloyd, G. R., Silwood, C. J., Grootveld, M., & Brereton, R. G. (2010). Supervised self organizing maps for classification and determination of potentially discriminatory variables: Illustrated by application to nuclear magnetic resonance metabolomic profiling. *Analytical Chemistry*, *82*(2), 628-638. https://doi.org/10.1021/ac9020566

Wu, X., Oldfield, P., & Heath, T. (2020). Spatial openness and student activities in an atrium: A parametric evaluation of a social informal learning environment. *Building and Environment*, *182*, 107141. https://doi.org/10.1016/j.buildenv.2020.107141

Xiang, L., Papastefanou, G., & Ng, E. (2020). Isovist indicators as a means to relieve pedestrian psycho-physiological stress in Hong Kong. *Environment and Planning B: Urban Analytics and City Science*. https://doi.org/10.1177/2399808320916768

Yang, T. C., & Matthews, S. A. (2010). The role of social and built environments in predicting self-rated stress: A multilevel analysis in Philadelphia. *Health & Place*, *16*(5), 803-810. https://doi.org/10.1016/j.healthplace.2010.04.005